CHALMERS

Investigation of a Variable Speed Wind Turbine and DC-Link Control for a Hybrid Power System

Thesis for the Diplom Ingenieur (FH) Degree

DANIEL TITTEL

Dept. of Energy and Environment
Division of Electric Power Engineering
CHALMERS UNIVERSITY OF TECHNOLOGY
Gothenburg
2007-06-27

Abstract

This thesis is about optimization of an existing wind-diesel hybrid power system in 30 kW power range having an intermediate direct current link.

The work will spot on several aspects of the system:

- Comparison of power sources other than wind power
- Passive versus active rectification and compensation
- Turbine Control
- Battery charging via DC-Link
- System Control
- Multi-Turbine Setup

Therefore, behaviour and control of the major components is to be studied. As there are: a pitched blade rotor, a permanent-magnet synchronous generator (PMSG), IGBT power converters and a PLC-control unit.

The task was to implement a new turbine and system control and setup new hardware. Therefore lab tests have been carried out at the Division of Electric Power Engineering at Chalmers University of Technology. As a result improved system behaviour could be achieved. Also the flexibility of the new system for different system configurations has been increased.
In addition some basic investigations on how to charge the battery via the DC-Link have been done. A setup for operating multiple turbines is proposed and built in the lab. By that, further tests can be accomplished in the future.

Keywords: DC-Link, wind energy, autonomous power systems

Preface

This work has been carried out at the Division of Electric Power Engineering at Chalmers University of Technology, Göteborg, Sweden in corporation with Pitchwind Systems AB, Lerum, Sweden from Oktober 2006 to June 2007.

The document further is registered as thesis work for the Diplom Ingenieur (FH) degree in electrical engineering for the University of Applied Sciences Mittweida, Germany.

I would like to thank my supervisor, Assoc. Prof. Ola Carlson who made it possible to stay at Chalmers and having support in different areas to carry out this work.
Further, I thank all the members of the department who always supported me, and gave me a great time here in Sweden.

As there was the connection to Pitchwind Systems AB all over our work, many thanks go to Mr. Lars Åkeson who was a great supervisor and taught us so much about wind energy in practice. Besides him, I enjoyed the company of my thesis colleague Dirk Dietrich as it always becomes easier if there are two heads that can think together.

Beside our work in Sweden, Prof. Ralf Werner in Germany has been a great help doing supervision at our home university the University of Applied Sciences Mittweida.

Finally, all this would not have been possible without the generous support of my family and my girlfriend who always were there if needed. For all your help I need to say:

Thank You.

Daniel Tittel
25th May 2007

Table of Content

List of Symbols

p	Number of pole pairs	[-]
R_s	Armature resistance	[Ω]
L_s	Armature inductance	[H]
Ψ_R	Rotor Flux	[Tesla]
T	Torque	[Nm]
Z	Impedance	[Ω]
ω_e	Angular electrical frequency	[rad/s]
ω_r	Angular rotor frequency	[rad/s]
n	Revolutional speed	[rpm]
r	Rotor diameter	[m]
l	Machine length	[m]
d	Machine diameter	[m]
B	Magnetic flux density	[T]
Φ	Magnetic field strength	[A/m]
E	Electric field strength	[V/m]
N	Number of turns in a winding	[-]
ü	transmission ratio	[-]
ρ	Air density	[kg/m^3]
v	Wind speed	[m/s]
λ	Tip-speed ration	[-]
C_p	Aerodynamic power coefficient	[-]
β_{pp}	Angle of attack, passive pitch angle	[deg]
β_0	Fixed pitch angle	[deg]
m	Mass	[kg]
E_{kin}	Kinetic Energy	[J]
F	Force	[N]
f	frequency	[Hz]
U, u	Electrical Voltage	[V]
I, i	Electrical Current	[A]
C	Electrical Capacity	[F]
P	Power	[W]
m_a	Modulation index	[-]

List of Abbreviations

A

AC	Alternating Current
AEP	Annual Energy Production
AR	Active Rectifier

C

CoM	Cost of Maintenance

D

DC	Direct Current
DTC	Direct Torque Control

H

HAWT	Horizontal Axis Wind Turbine
HCPV	High Concentrated Photovoltaic
HPS	Hybrid Power System
HVDC	High Voltage Direct Current (Transmission)

M

MAC	Media Access Control

I

INV	Inverter
IPC	Industrial Personal Computer
IP	Internet Protocoll

O

OWEC	Ocean Wave Energy Converter

P

PF	Power Factor, cos(phi)
PFC	Power Factor Correction
PI-	Proportional/Integral (regulator)

PMSG	Permanent Magnet Synchronous Generator
PM	Permanent Magnet
PLC	Programmable Logic Control
PV	Photovoltaic
PPT	Power Point Tracking
R	
RMS	Root Mean Square
S	
SWEC	Small Wind Energy Converter
SPL	Sound Pressure Level
SOC	State of Charge
T	
TCP	Transmission Control Protocol
V	
VAWT	Vertical Axis Wind Turbine
W	
WEC	Wind Energy Converter

1 Introduction

1.1 Why Hybrid Power Systems are needed

Large volumes of electrical energy are required to develop a modern society, thus, global energy consumption is expected to double for the next 30 years [1] as the number of global population rises. Lots of indicators show that there will be a great demand for renewable energy right now as in the future, due to various environmental concerns taking place in different regions on our planet or being predicted by scientists. The most important ones are in fact known for a long time, but became much more present with the latest world-wide catastrophes due to an ongoing change in climate.
Of course, there will also be an end of fossil energy resources, but the latest investigations estimate, that we will face these problems not before the mid of this century [2].

Despite the far future and starving of fossil resources, economical studies [3] show also, that there will be a tremendous future increase in price for raw material, meaning that the production of energy by the use of most expensive fossil resources in future times will result in an unfavourable economical balance.

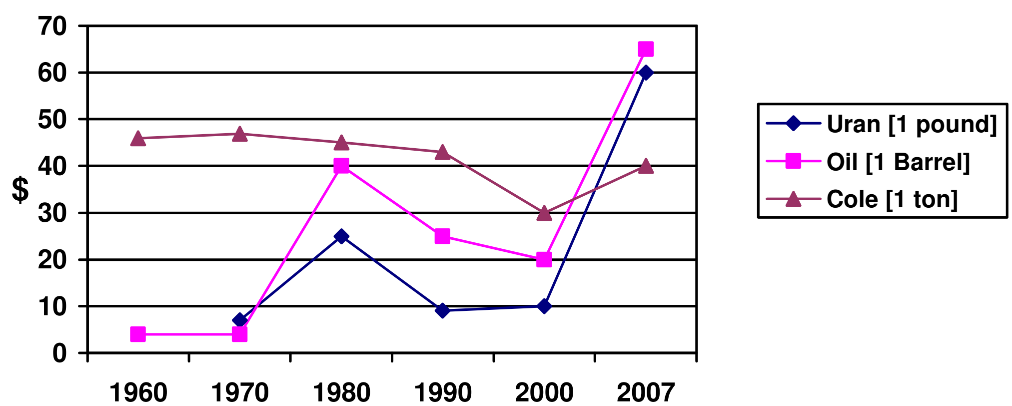

Figure 1.1-1 Historical price charts for different fossil resources, Sources: [4], [5], [6]

It should be mentioned clearly - success of renewable technologies today is not a question of ecological techniques with an appealing "nice-to-have" attribute but a question of financial cost in a strongly competing energy market. Figure 1.1-1 shows that the edge is coming to alternative energy resources as prices for fossil resources rose to a large extend during past years. Unfortunately, we still do not speak about the "expense of energy" but the "cost" of this very special good. The difference might be considerable.

Also, not many people are aware of the number of people living without electricity being not yet connected to any energy source. Two billion people live without access to electricity. Most of those people usually live in poor and remote regions and have almost no possibility to catch up with modern societies. Solid and reliable island grids are seriously needed without financial and ecological drawbacks to not make the people dependent on these.

Regarding wind energy as the solely solution of present and future problems could easily mislead, it should be perceived, that new technologies enter the market and therefore the role of wind energy must be reinvestigated in certain periods. Why should we keep on working on wind energy converting devices if better technology is available? How perform other technologies nowadays? In fact, basic knowledge about the existing wind-diesel system has been mainly collected from 1987 until 1999 [7], [8], [9] at Chalmers University of Technology. Therefore chapter 3 will show a performance comparison of the used wind energy converter (WEC) with a competitor and other latest renewable technologies.

Even though, some more expensive components can be a good choice for building autonomous hybrid power systems (HPS) used in autonomous regions. The following two pictures demonstrate two scenarios and try to give some explanation:

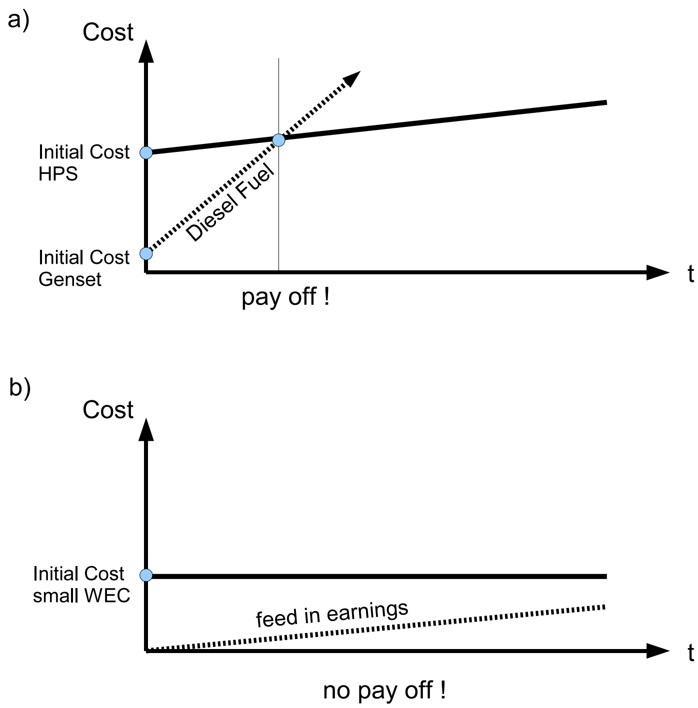

Figure 1.1-2 Pay-off Comparison a) HPS vs. Diesel Genset b) Grid connected WEC

Regarding Figure 1.1-2 a) in an autonomous power system, the cost of diesel fuel for a standard genset will quickly raise and surpass the running cost of a wind-diesel system. In contrast figure b) shows that feed in tariffs are not enough to pay off for a small grid connected WEC in same size. No other fact than this can be named as a reason for building hybrid power systems

For a basic approach in developing hybrid power systems, the following major aspects should be regarded when estimating the usage of wind energy:

- We are facing serious climate changes that could affect components
- Fossil resources will become short
- Prices for extraction of fossil resources will increase tremendously
- Existing renewable techniques are developed steadily
- New renewable techniques enter the market

1.2 Outline of Thesis

Chapter 1 includes a short introduction to Hybrid Power Systems.

Chapter 2 deals with basic facts in wind energy. The chapter's purpose is to provide some background to wind energy in common.

Chapter 3 shows a comparison of different sources for hybrid power systems. Due to very different locations were hybrid systems like to be placed, some key parameters of different technologies have been investigated. By that, future decisions on different power sources other than wind power should be made easier.

Chapter 4 will carefully look at the Pitchwind Hybrid Power System itself. The system setup and the system principle are described. In the sub-chapters, discussion on major components can be found and the new turbine control loops will be presented. It will also touch the topic of charging batteries via the DC-Link and show how multiple turbines could be controlled. Further it will deal with the development of a new control system using Modbus/TCP.

Chapter 5 contains measurements proving the function of the new system and control.

Chapter 6 will summarize the results of this work and give some conclusions as well as an outlook to future work

Appendixes A, B will provide further data and schemes not presented in the chapters.

2 Facts in Wind Energy

While this thesis will investigate aspects of a wind-diesel system, some efforts have been put to present the current situation of wind energy. As the original background of the author is communication technology it just seems to be consequent to look at certain aspects of renewable and wind energy production in general.

2.1 CO_2 Emissions of power production

For sure, one convincing argument of wind power is low emission of carbon dioxide. Beside the 23 times more effective methane (CH_4), carbon dioxide (CO_2) is the most important greenhouse gas as it simply dominates by huge volumes of emission [10], [11].

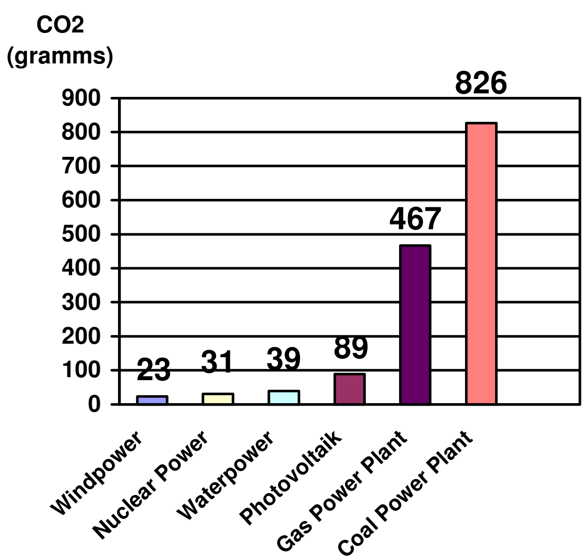

Figure 2.1-1 Comparison of CO_2 Emission for production of 1 kWh [12], [21]

2.2 Is wind power economically competitive?

In February 2006, for the very first time, the traded price for wind energy at Leipziger Strombörse EEX[1] was lower than the price of regular power from traditional power plants. On 10th of March 2007, there was more energy produced by german wind power than by all nuclear power stations together. These facts indicate, in future times wind power could help to make energy cheaper. As many energy suppliers became aware of this fact, they are strongly focussing on building new wind-power capacities all over Europe.

If we further focus on island hybrid power systems, the impact of renewable energy sources shows high savings in diesel fuel. Depending on the system location, the diesel generators can be shut off up to 80% of the time [13]. Small diesel generators usually can not be run at high system efficiencies. They often provide poor load regulation. The replacement by small wind-diesel systems indicates the economical break-even after approximately 4 years [13].

2.3 Worldwide wind-power market

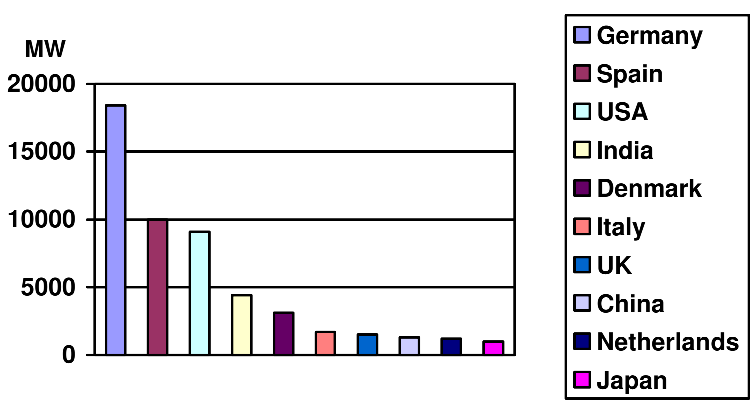

Figure 2.3-1 Top ten nations' installed wind power [14]

[1] EEX – European Energy Exchange, trades energy contracts since year 2002

The graph shows that wind power is becoming a worldwide issue. Still, Germany keeps the top position when it comes to totallyl installed wind power.

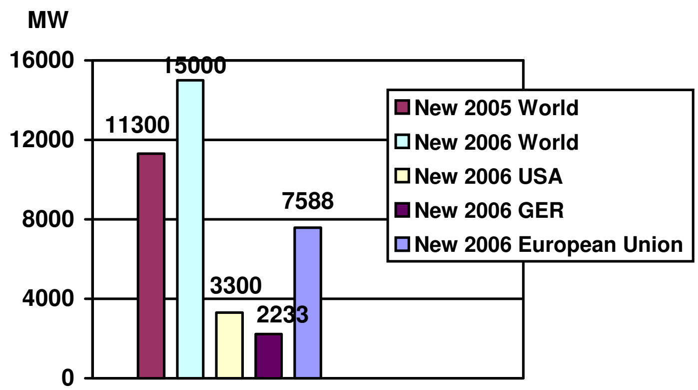

Figure 2.3-2 Comparison of new installed wind power [14]

Figure 2.3-2 shows, that the pioneering German wind market has slowed down and will be overtaken by the US American market in the future. Both countries have high carbon dioxide emissions and seem to see the opportunities wind power haves.

The latest political discussions indicate that many industry nations aim to reduce their overall emissions. New investments in off-shore technology could really contribute to cover more electricity generated by wind power. Nevertheless, new wind power capacity will ask for new backup capacity in the grids. Therefore intelligent power management and highly cross-linked grids are necessary. How much wind power contributes in some countries today is illustrated below.

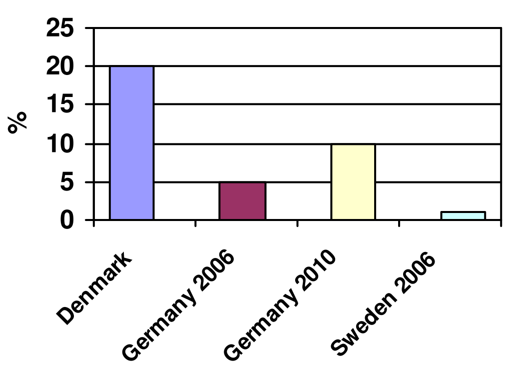

Figure 2.3-3 Wind power contribution in European grids [15], [16]

Figure 2.3-3 can not be left without a comment – Denmark's high wind power contribution is only achieved by the connection to the Norwegian power grid which acts like a big battery in case many Danish turbines have to shut down.

2.4 Global consumption covering

In 2004, wind power production was estimated to 104 TWh of electrical energy, this covers for 0.6% of the global energy consumption [17].

2.5 Trends in Wind Energy

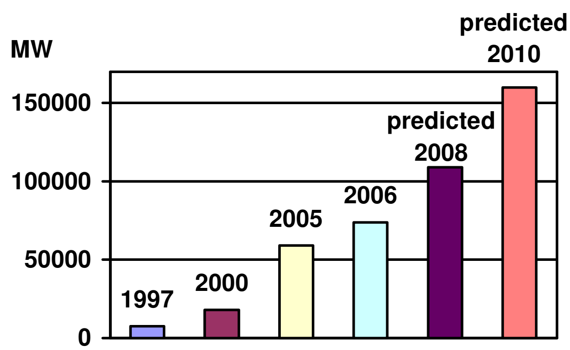

Figure 2.5-1 Worldwide installed Wind Power and Prediction [18]

The prediction shows further growth for wind energy, but it should be pointed out, that this growth will be mainly driven by countries like USA, China, India or Brazil. As the last named countries are much into manufacturing industry, the energy demand will be especially high for the next time, thus, all these countries set up new political strategies for new wind power systems.

In contrast to the promising figures many european on-shore markets are almost saturated and now ready for so called "re-powering". Further on, there is a driving force to erect large and much productive off-shore parks as the energy production for almost the same type of wind-turbine can be doubled due to higher wind penetration.

Finally a short overview of some recent trends shall be given below:

- **Re-Powering** is a trend of replacing older WECs by the latest turbine technology with higher towers and larger rotor-diameters. Often this includes new frequency power inverters too, as they are friendlier in turbine control towards the grid.
- **HVDC Transmission,** by the help of new High-Voltage-DC transmission techniques, transport losses from remote locations can be reduced. It is aimed, to reach losses of 3% each 1000 km.
- **High-Towers** can be used to reach lower atmospheric streams. By that, the energy production of WECs can be extremely increased at some locations. Also common on-shore locations can benefit by the application of high towers. The world’s highest tower is currently erected in Laasow (Brandenburg, Germany) and will reach 160 metres in high.
- **Off-Shore Parks,** although well known for a long time, off-shore solutions are still not common. Due to comprehensive investigations on effects to sea live and careful investors most off-shore parks are still in state of planning. It is shown, that off-shore sites can give twice the energy production of common on-shore sites but also increase installation costs to a big amount.
- **In-Built Maintenance Units** address the call for low maintenance cost. The nacelle has an in built crane and easy detachable components for maintenance purpose.
- **Various Blade Sizes for one Turbine,** as turbines of the same power range are erected on different sites with different conditions, it just seems logical to offer different blade sizes for different average wind-speeds.
- **Full Inverters,** due to higher power-quality demands from grid operators, it is appropriate to use full inverters, as they can provide full load and grid control by supplying enough reactive power.
- **Super Capacitors** are used to act as power backup in turbine failure scenarios to support the pitch-mechanism to reach safe operation mode.

3 Basic Comparison of Renewable Energy Resources

This chapter will try to give a basic comparison of renewable energy resources. Basic facts about competing techniques are shown, at least to get a general idea of some aspects that might be important to know when it comes to engineering in the field of renewable energy and combining various renewable power sources for a hybrid power system[1].
Also, the comparison will show how competitive a small scale wind system versus common large scale systems performs. It is also aimed to find another small WEC in the same power range to the existing Pitchwind WEC. By doing this, alternatives should be found that could replace the actual wind-turbine. The comparison is not ought to give comprehensive financial analysis.

To do a comparison though, some boundaries have to be found:

1. The final power output needs to be of electrical energy
2. Biomass energy is not regarded
3. Fuel-Cell technology is not regarded, as the problem of reliable hydrogen supply and storage is not solved yet
4. Geo thermal energy is not regarded, as there are too specific aspects of site selection to make common economical use of it
5. Only solutions that are "ready-to-market" are regarded
6. Technology must be capable of producing at least 25 kWp[2] and able to be clustered
7. Only recent commercial systems of each category are compared
8. Each technology is operating at its specific, preferable site
9. As cost of operating and maintenance (CoM) are estimated to be roughly equal for all technologies - except photovoltaic (PV), this quantity is not taken into account for comparison

---

[1] Aspects on batteries for hybrid power systems can be found in *Backup Energy and Supply Side Investigations of a Hybrid Power System, Dirk Dietrich, 2007*

[2] kW peak, power that can be achieved by maximum penetration

10. Expected product lifetime seems to be close the same (approx. 20 years) or is very hard to estimate precisely for all presented technologies, therefore it is set to be equal

As these assumptions are made, they lead to the following technologies that can be compared:

A. Wind energy converter [3MW] (WEC)
B. Photovoltaic (PV)
C. High Concentrated Photovoltaic[1] (HCPV)
D. Ocean wave energy converter [750kW] (OWEC)
E. Small wind energy converter 1 [30kW] (SWEC_1)
F. Small wind energy converter 2 [25kW] (SWEC_2)

For the comparison, the following real-life systems were chosen:

A. Vestas V90 3 MW, offshore (WEC)
B. Solarworld SunModule Series, silicon thin film (PV)
C. SolarSystems CS500 Modules[2] (HCPV)
D. Ocean Power Delivery Pelamis (OWEC)
E. Pitchwind PW30/14, 30 kW (SWEC_1)
F. Eoltec Wind Runner E11-25, 25 kW (SWEC_2)

Now, one still has to choose expressive quantities to compare the performance of these four chosen technologies.

First quantity is the annual energy production on one square metre of occupied area. It represents a kind of energy output density of each compared technology.

A second and exciting quantity is the time of energy amortisation of each technology. By that the time will be given for which the technology is able to produce as much energy as had been needed for its production and erection.

---

[1] HCPV can be realized by applying Fresnel-lenses in front of the PV-cells or by using large mirrors focusing the sunlight to a central point.

[2] Uses large mirror discs, also known as heliostatic concentrators

Next quantity will be the simplified cost for 1 kWp installed. This will give an impression on how much money has to be invested to install a certain size of technology.

An important measure but difficult to determine value is the cost for one produced kWh. Only this quantity will give the true performance of a certain technology. The comparison therefore includes a simplified cost per 1 kWh.

As the "not-in-my-backyard-problem" is not negligible, the emitted noise level is taken into comparison, too, and will be the last quantity compared.

Again, all comparable quantities and their units:

- Annual energy productions per area $\left[\frac{kWh \cdot y}{m^2}\right]$
- Energy amortisation time $[years]$
- Simplified Cost per 1 kWp installed $\left[\frac{EUR}{kWp}\right]$
- Simplified Cost for 1 kWh $\left[\frac{EUR}{kWh}\right]$
- Noise level $[dB(A)]$

3.1 Annual Energy Production per area

To do an objective comparison, a table with preferred locations of each system is provided. As defined in Assumption 8 the most preferable site for each technology was chosen to show best possible performance. The reason for doing that is in turn the consequence of choosing the most appropriate technology for a supposed installation place.

Technology	Location
Vestas V-90 3MW (WEC)	Scottish Coast, Offshore, UK
Photovoltaic (PV)	California, USA
HC-Photovoltaic (HCPV)	Victoria, Australia
OPD Pelamis (OWEC)	Atlantic Ocean, Portugal
Pitchwind System (SWEC_1)	Estland, Onshore , close to sea
Eoltec System (SWEC_2)	Estland, Onshore, close to sea

3.1-1 Preferred sites for the chosen technologies

It needs to be said, that in most cases these preferred sites surpass annual energy production of an average site approximately twice.

For calculating the ratio of energy production per square meter, the footprint for every technology is needed. To find the actual needed area, the minimum footprint (allowing safety margins) for clustering the technology was determined and taken for calculation.

The collected numbers can be found in *Appendix A* and lead to the following graph:

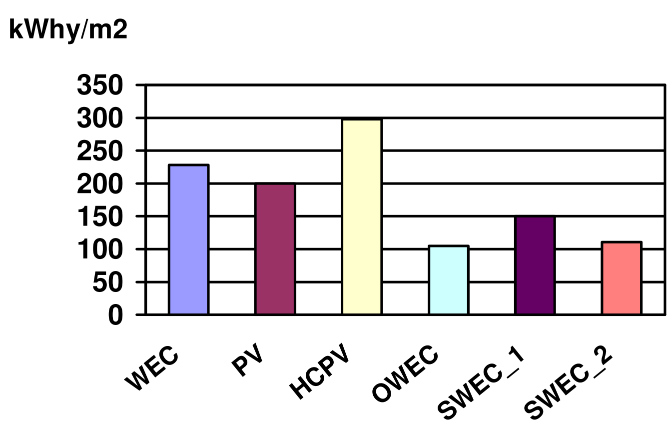

Figure 3.1-1 Comparison of annual energy production per 1 m^2 reserved footprint

As the graph shows, the HCPV produces the most annual energy per area. As it makes use of very close clustering and higher efficiencies compared to PV technology it leads the comparison. Second highest output per square meter is being achieved by the WEC technology. Somewhat unusual is the bad ranking of the OWEC. Because of the different media properties the energy being recovered should be very high for the OWEC. Due to the much higher density of water related to the relatively slow wave propagation speed, the amount of present energy per 1 m^2 of area is usually higher than what we could obtain in 1 m^2 wind area. Unfortunately, the OWEC does not allow a close clustering due to some safety issues. Though, looked on a single unit, the OWEC remains as a very effective device.

Another aspect is the gap between the big WEC and the smaller SWEC_1 and SWEC_2. This is mainly caused by a bigger area passing upper wind streams. Also, big WEC systems achieve higher system efficiencies than small scaled systems, mainly in terms of high aerodynamic- and generator efficiencies. Most important in terms of annual energy production between different wind technologies remain the local site conditions. Therefore the comparison of WECs on different sites can not give clear answers.

3.2 Energy Amortisation Time

As the there are no data acquired for OWEC yet - the author assumes a poorer energy amortisation time of the OWEC in comparison to the large 3MW WEC. As one OWEC reaches only 1/5th of the annual energy output of one 3MW WEC the amortisation time is estimated to be five times higher as used material weight and installation expenses are roughly equal. But, for future discussion the learning curve for the OWEC technology should not be neglected as the presented device is the first commercial available product on the market. Unfortunately, as the SWEC_1 and SWEC_2 are not produced in serious mass-production and no data are given, estimation cannot be done. The same lag of information is for the HCPV System.

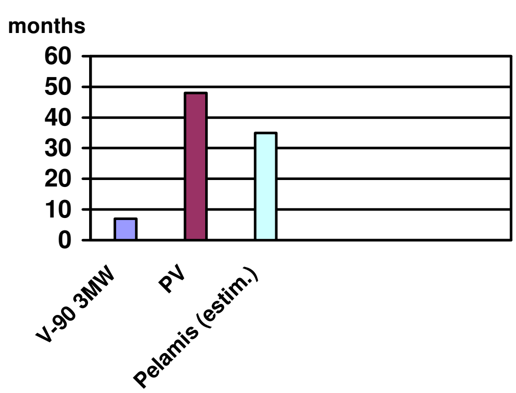

Figure 3.2-1 Energy amortisation of each technology [19], [12]

3.3 Simplified cost per installed kWp

The simplified cost per 1 kWp does not include any cost for real estate or shipping. The quantity only expresses the cost for acquisition and erection of each technology and should help the system designer to quickly get an image about different market prices.

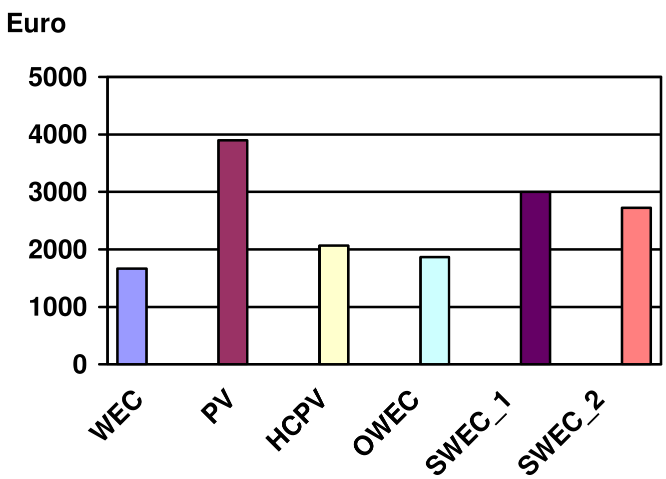

Figure 3.3-1 Net-Cost per installed 1 kWp of each technology

The graph above shows the lowest cost for the WEC technology. Almost equal results can be seen by the OWEC technology which is supposed to pursue a steep learning curve in the next years.

As commonly known, the cost for a small wind energy system is much higher than for a large scale system. This originates from very low production volumes and cost-scaling-effects arising by building bigger systems. Even though, the SWEC_2 shows better economic performance to SWEC_1. Obviously it could be a good choice to be used in a hybrid power system.

One impressive fact is the stability of high prices for PV systems. A new study [20] of the RWI Essen shows, that the feed-in rates are too high and do not force the suppliers to lower PV-module prices. Due to the high demand - module prices remain at levels seen in 2001. A change on international feed-in policies could lower prices to a certain amount.

Nevertheless, one remarkable advantage of PV-systems is the very low requirement of maintenance compared to all other technologies, due to that, the high investment costs can equal out in operation over a long time.
Most exciting will be the continuous introduction of HCPV technology. It seems that this technology aggressively tries to cut down costs. Therefore it could become an option for classic wind-diesel hybrid power systems.

3.4 Simplified cost per produced kWh

The author is aware, that serious cost calculation is serious work and dependant of many variables that cannot be determined in short time. Usually, a long data-acquisition-process is necessary to determine real cost per one produced kWh of each technology and over whole life-time.

As there is only few reliable data for CoM (Cost of Maintenance) calculations available, too many factors make calculations difficult. For example local site conditions and local cost of workforce or shipping cost affect serious CoM numbers quiet much. Further, it is hard to determine the remaining value of used systems being replaced after a certain time. The case of replacing old systems by better current systems is often disregarded but quite common in real.
Literature research showed that life-time expectations of each technology can be averaged to be all the same. No recycling technologies are included either, as there are new proceedings shown by the PV-industry for example. This would affect investment costs and investment planning additionally.
For that reason a CoM comparison and a real cost per kWh calculation are not been carried out.

To do such a calculation we again need to find some assumptions:

- life time for all systems is assumed to be 20 years
- the terminal value after 20 years of use is set to zero
- the annual energy production (AEP) is equal for every year of operation
- System Cost will be reduced to the simplified technology cost

Now it can be calculated as follows:

$$SimpleCost_{1kWh} = \frac{SystemCost}{20\,years \cdot AEP}$$

Eq. 3-1

By applying the numbers provided in *Appendix A* we will come to the following graph:

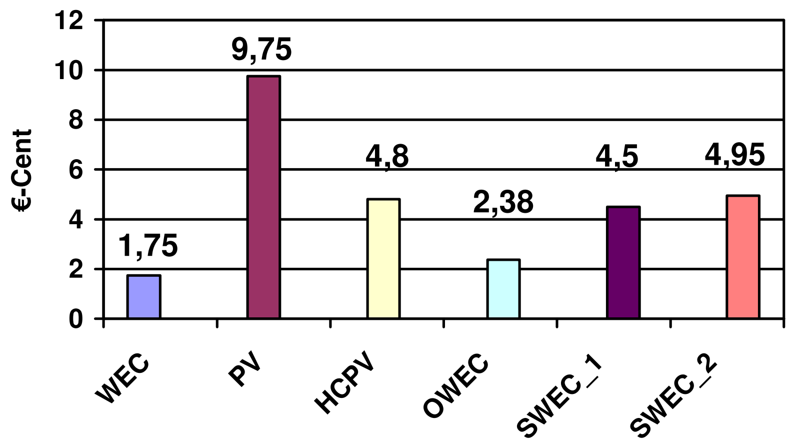

Figure 3.4-1 Comparison of Simple Cost per kWh

It can be seen, that the WEC is leading the comparison with lowest costs. Surprisingly well performs the OWEC. It seems that this technology could have a bright future if the cost in mass production can be even lowered, a strong competition against expensive off-shore farms could be a consequence.

Due to high costs the PV technology produces expensive electricity. The just started HCPV technology definitely will get in strong competition with the classic PV. By the matter of time it could dominate the future market if no better PV technology is developed. Still one has to consider that HCPV is on the very beginning and will seriously have to prove its abilities in long term usage.
So far, PV systems usually will remain too expensive to be used in common hybrid power systems.

Due to a smaller rotor diameter SWEC_2 produces less energy and therefore has somewhat higher costs for one produced kWh than SWEC_1 has. As the maintenance of SWEC_2 is supposed to be much lower it still could be a better choice.

Regarding Figure 3.3-1 and Figure 3.4-1 apparently there is a correlation between the simplified cost of installed kWp and simplified investment cost per kWh. One could summarize, that expensive technologies have higher costs for each produced kWh. Again, it should be mentioned that including any additional costs can change the real cost by far.
As always for this comparison, we cannot select one technology as “the winner” as specific regional climate conditions predict the use of different technologies. Despite that, the investigation shows remarkable potential for a wider choice of alternative power sources used in the future.

Best opportunities in a future competition seem to have:

- WEC
- OWEC
- HCPV

These technologies show either very good performance or have a steep learning curve to follow that will put them closer to the leading wind power technology.

3.5 Noise Level

Measuring noise level is merely an issue for WECs and OWECs as PV technologies are almost totally quiet[1].

In fact, measuring noise level is not so easy, as at some distance from our noise source the emitted and surrounding noise-level can barely be distinguished.

As the Pelamis OWEC only consists of slow moving mechanical parts and moves with the waves the emitted noise level is assumed to be very low. Further, the background noise off-shore is somewhat higher than background noise on-shore. Additionally, distances between operation and on-shore places are so high, that audible noise-impact is assumed to be neglect able small.

---

[1] converter noise is neglected, even thought they can emit strong high-frequency noise

This is not the case for WECs as at higher wind speeds and power levels two noise sources begin to develop. On the one hand there will be noise from turbulences due to the blades and an optional gear-box. On the other hand the wind itself will start to increase the present background noise.

The worst case will be experienced around 12 m/s wind speed and approximately 95% power level [29]. At that point surround noise and emitted turbine noise will be most apart to result in high noise heard from the turbine. Latest wind turbine developments show almost no tendency to single tones, while serious infrasonic tests are not undertaken yet. As we look at off-shore installations, the impact on sea-mammals could be not negligible.

Noise levels are usually expressed as sound pressure levels (SPL) and suit well to the human perception of sound. The SPL is defined as the relation of an actual air pressure level p_1 to a reference air pressure level p_0.

$$SPL(dB) = 10 \cdot \log_{10}\left(\frac{p_1^{\;2}}{p_0^{\;2}}\right)$$ [1]

Eq. 3-2

If we know the SPL for a noise source it is possible to calculate the noise-level at a certain distance by using the fact, that a certain sound pressure level decreases indirect proportional to the distance. Sometimes this rule is called 1/r rule.
An implementation of this calculation method was found in the "Sound Map Calculator" from the DWIA [29] where a local noise-distribution can be displayed on a virtual area without any obstacles.

First, a maximum permissible sound level of 45 dB(A)[2] is defined [29]. According to industry standards the maximum noise level for a WEC is measured at a wind speed of 8 m/s in 10 metres of high. For the WEC this value is 100 dB(A)[3][29] the SWEC_1 reaches 98dB(A) which had been measured by [22].
In the coming figures each square represents a distance of 50 metres.

---

[1] $p_0 = 2x\ 10^{-5}$ Pa

[2] Note: Maximal sound-level for houses in Sweden is 40 dB(A), general living area Germany 40 dB(A)

[3] dB(A) - A-weighted with a filter-curve similar to the human ear perception (see Appendix A)

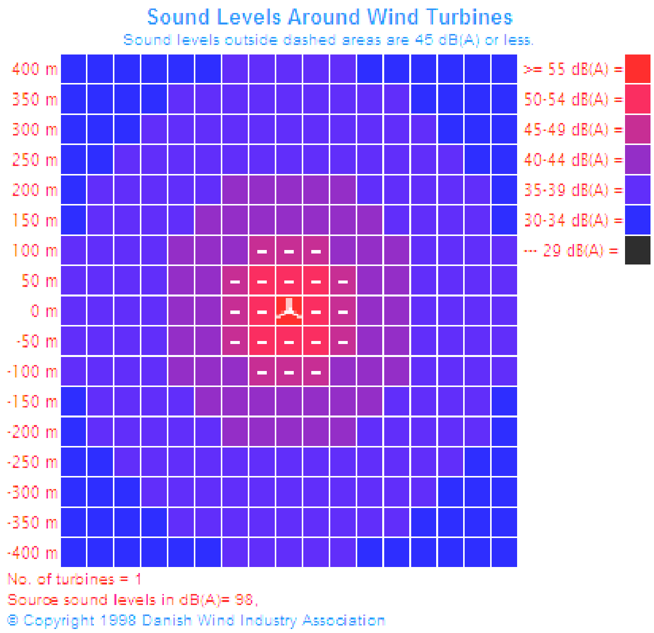

Figure 3.5-1 Sound Level Distribution for one turbine 98dB(A) – dashed squares indicate levels above 45 db(A)

From the figure above we can see, that the sound level will be below 45dB(A) after more than 100 metres. If more turbines are being operated the linear sound levels can be just added what will lead to a minor effect on a logarithmic scale. The picture below demonstrates this for three SWEC_1 turbines set up 150 metres from each other:

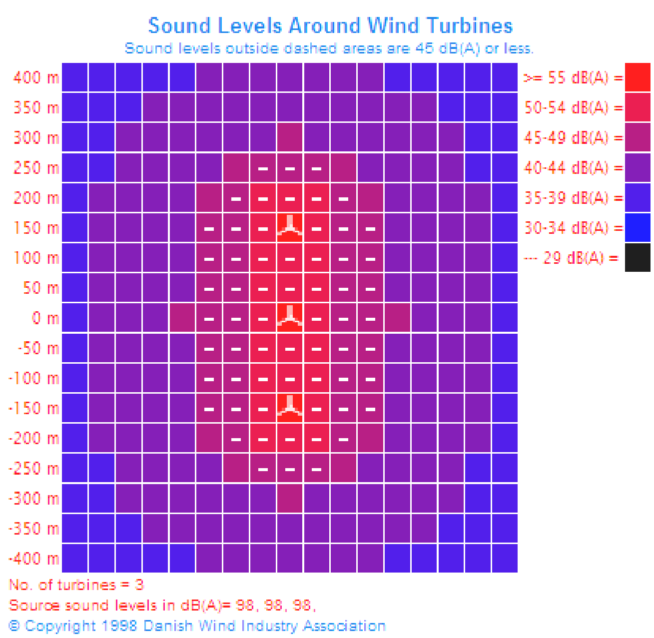

Figure 3.5-2 Sound Level Distribution for three turbines each 98dB(A) – dashed squares indicate levels above 45 dB(A)

The figures show, that the distance does not need to be increased so much to stay below the maximum noise level of 45 dB(A).

By these graphs it is proven that modern turbines do not affect the live-quality even if they are erected close. If interested people are concerned about noise-levels of the WEC used for the hybrid power system there should not be concerns any longer. A distance of more than 100 metres for the SWEC_1 should be kept for safety reasons in any case.

4 Hybrid Power System

4.1 Hybrid System Overview

Basically, the current system consists of the following major components:

- Wind Turbine
- Generator (PMSG)
- Active Rectifier (AR)
- Grid Inverter
- Batteries (lead-acid type)
- Charger
- Diesel Generator
- PLC (Programmable Logic Control)
- Transformer (optional)
- Filters

The following picture shows how all these components are connected and how they form the hybrid power system:

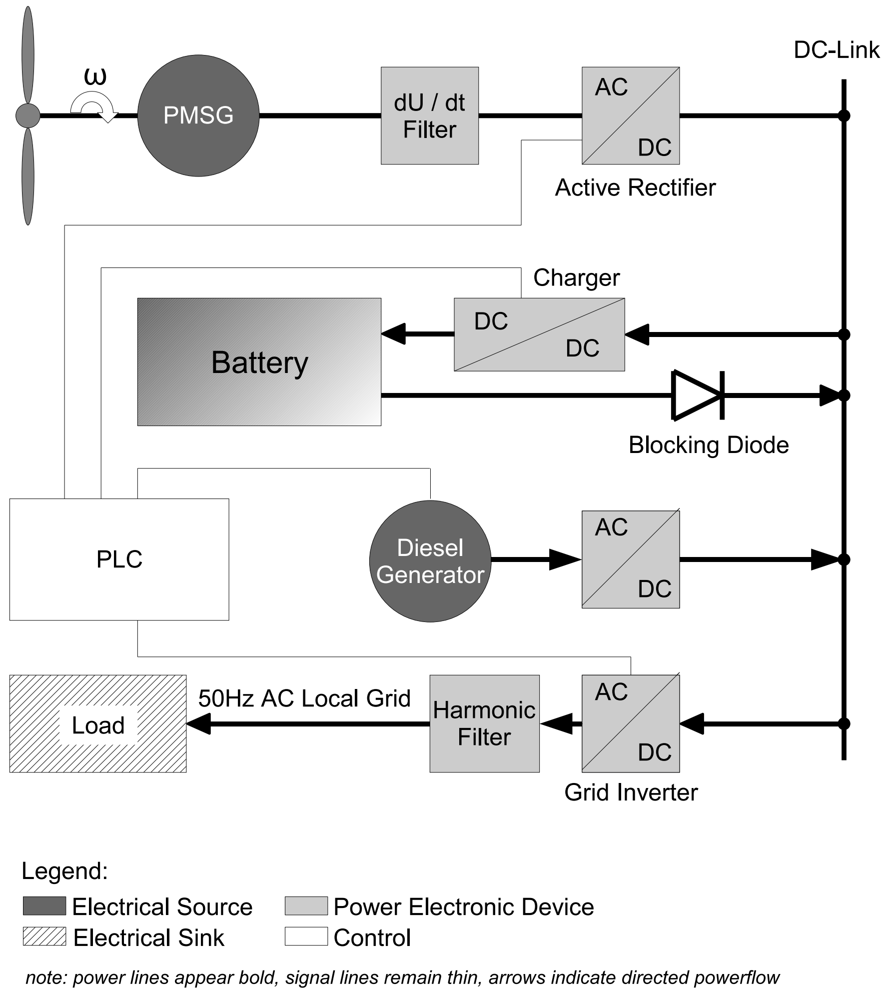

Figure 4.1-1 Overview about the system configuration of the hybrid power system (HPS)

As this thesis is dealing only with some components of the system, the function of considered devices is presented in the following sub-chapters.

Due to the actual situation, components of the system needed to be changed. This had been caused by discontinued components and new demands to the systems flexibility.

The following picture encircles the components being changed and needing new attention:

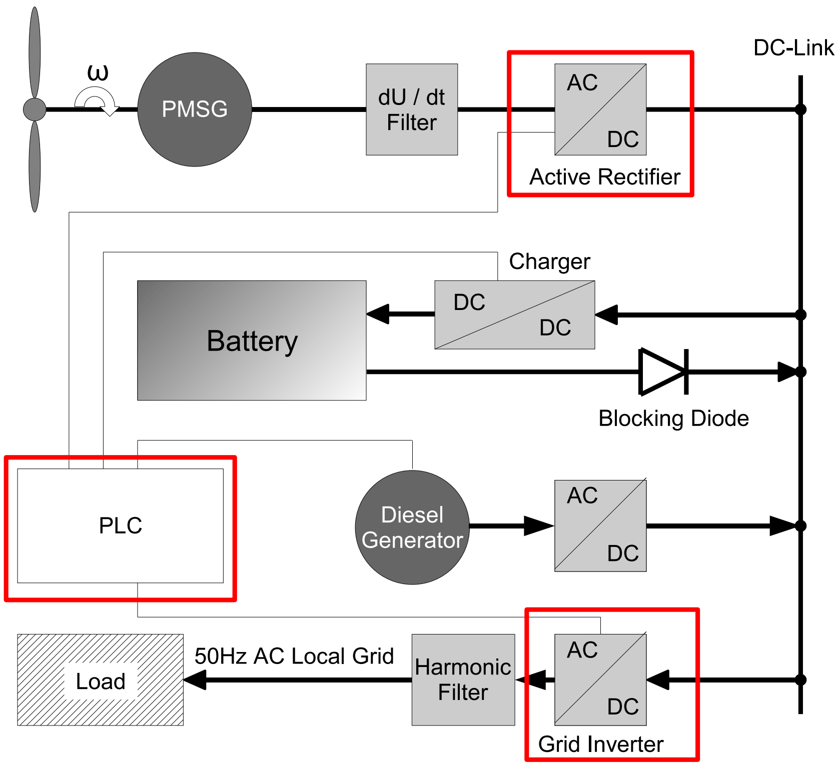

Figure 4.1-2 Indication of components that are replaced in the actual HPS

Before implementing and testing new control software, the components need to be studied.

For testing purposes an experimental setup has been built up which is able to operate the components as in real life systems. Excluded in these tests were the charger, the diesel generator and the harmonic filter.

4.2 Hybrid Power System Operation

Many components can be found in a HPS: How do these components all work together? Basically, the answer is: Any load-situation at the HPS can be managed by controlled operation of the DC-Link.

To see how this works, the HPS is presented more simplified and some example values are given in the figures. Also there a two small graphs, one showing the turbines power curve and a dot that is indicating the operation point, another showing the DC-Link voltage. For explanation purpose, three scenarios are developed.

SCENARIO 1:

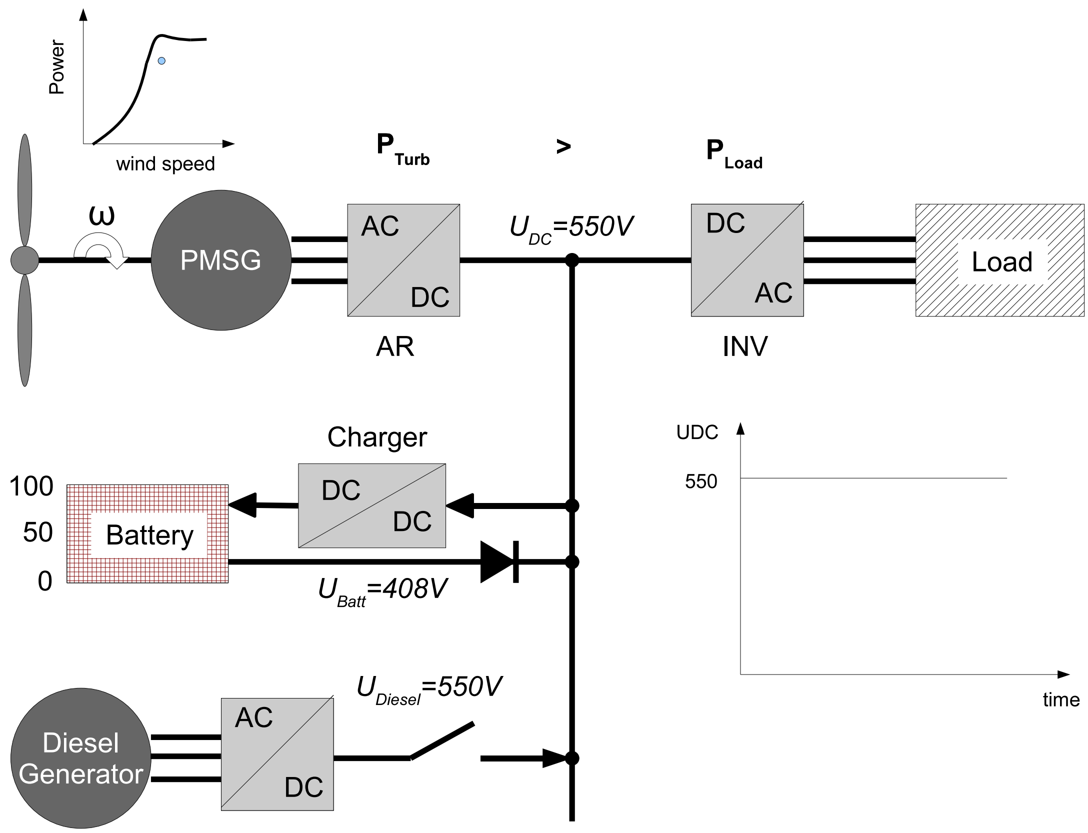

Figure 4.2-1 HPS Principal – Scenario 1

In scenario 1 we face optimal conditions for the system. The demanded load from the grid P_{Load} is lower then the power present in the wind and further the turbine power P_{Turb}. Therefore, the AR will be able to control the UDC voltage at the preferred level of 550V. As can be seen from the small chart in the upper left corner, the turbine is operated at an operation point below the actual wind power. By that, the turbine will start to spin faster due to the low-load condition. Over-speed will be prevented by the passive pitch mechanism of the turbine. The battery has a 100% state of charge (SOC) but will not interact as the blocking diode prevents any power flow towards the DC-Link. The diesel generator is shut off.

SCENARIO 2:

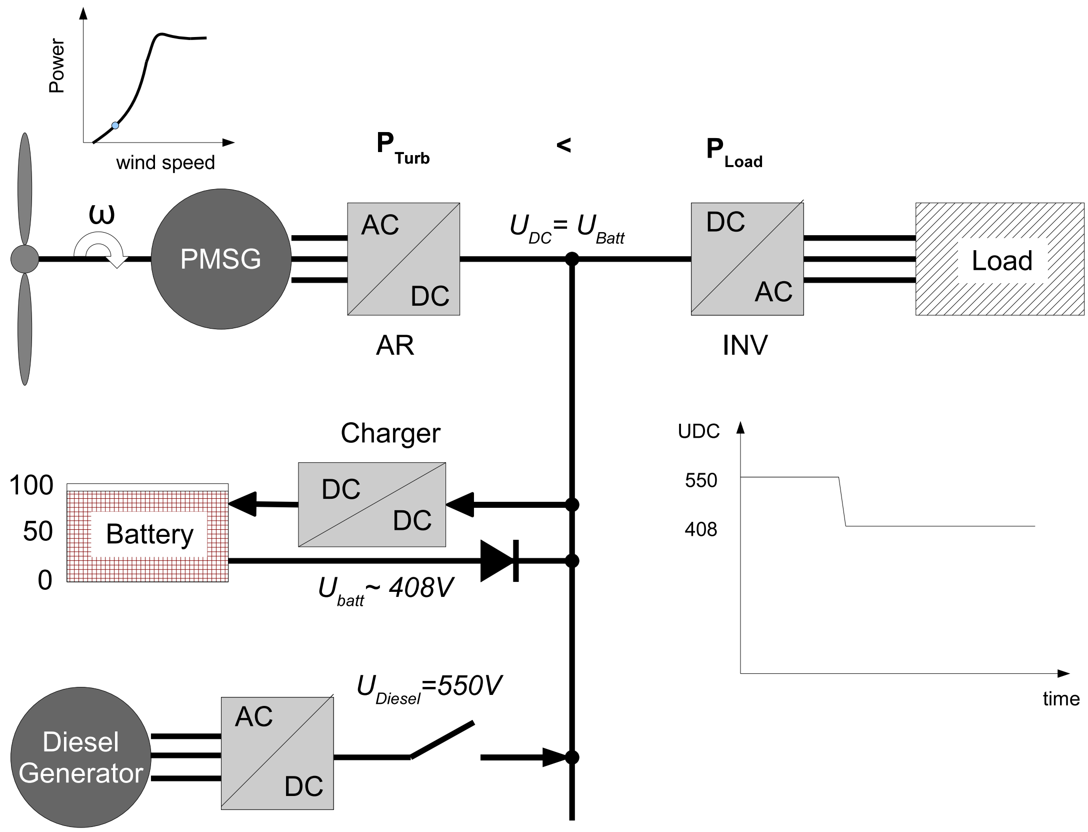

Figure 4.2-2 HPS Principal – Scenario 2

Scenario 2 is much different as the demanded load is higher than the present turbine power. Having that situation, the AR will not be able to sustain the adjusted DC-Link voltage. Immediately, the UDC-level will drop – until it touches the 408V battery voltage level. In case the voltage difference exceeds the forward voltage of the diode, suddenly the INV will be supplied by the backup batteries which suddenly begin to discharge.
If the batteries cannot be recharged by wind power again and reach a specified low SOC, we will finally reach scenario 3.

SCENARIO 3:

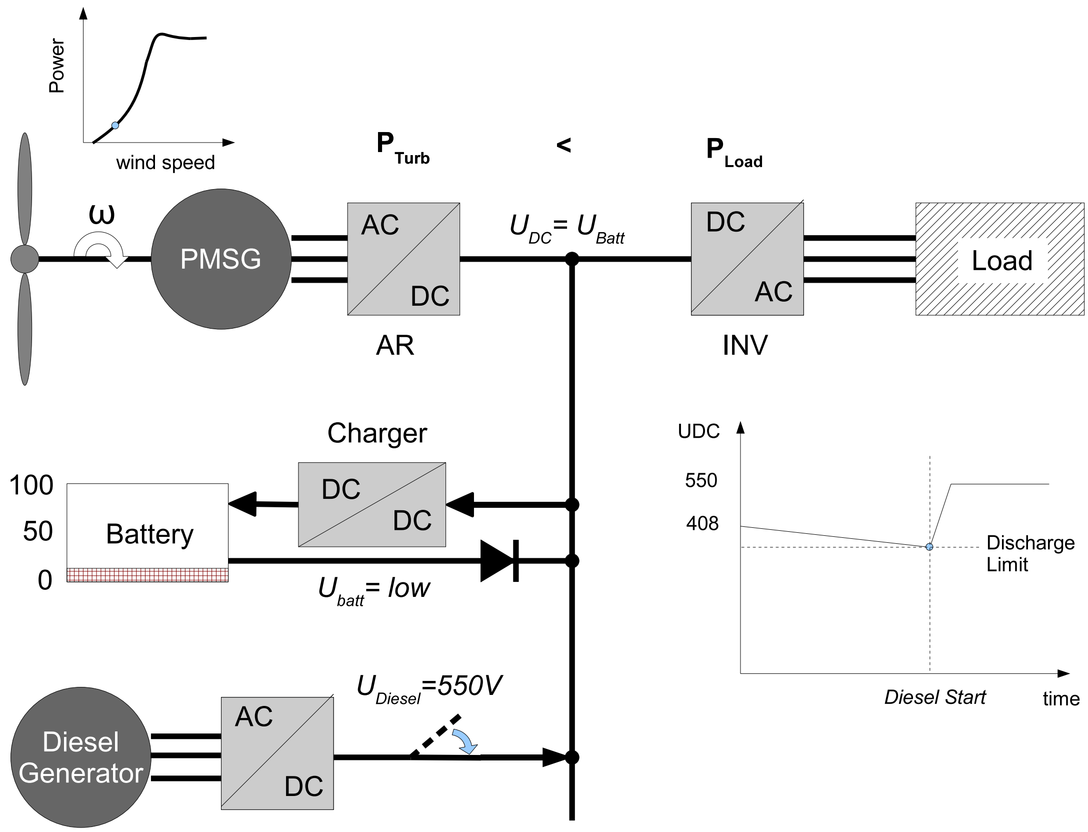

Figure 4.2-3 HPS Principal – Scenario 3

Obviously, the adjusted battery discharge limit is reached and the diesel generator has been activated. By closing the contactor the generator feeds the DC-Link now. At the same time there will be a command for the charger to charge the battery. If the batteries reach 100% SOC again the diesel generator will be disconnected and switched off.

4.3 Rotor

As the Rotor plays a major part to get any energy out of the wind, it is worth to take a closer look at the applying principles. Actually it should be said, the main control task on a wind turbine will always be to control the rotor in a suitable way.

4.3.1 Power in the Wind

A wind turbine basically can be described as a power transformer. It transforms almost linear kinetic wind energy into rotational kinetic energy in a first step and finally will convert this into electrical energy. These transformations are mainly achieved by two helpers, the rotor blades and the generator. To see how effective this conversion can be done, the present energy of the wind needs to be determined first.

Actually, the energy carriers are small air particles with a mass *m* and moving velocity *v*. Doing the assumption that all particles at different locations in space have the same motional speed before hitting the rotor, we find the following equation:

$$E_{kin} = \frac{1}{2} m \cdot v^2$$

Eq. 4-1

By substituting the particle mass with air density, wind speed, time and applying a circular crossing area with radius r we can express the wind energy facing a virtual rotor disc, as following:

$$m = \rho \cdot V = \rho \cdot A \cdot v \cdot t = \rho \cdot \pi \cdot r^2 \cdot v \cdot t$$

Eq. 4-2

$$E_{wind} = \frac{1}{2} \cdot \rho \cdot \pi \cdot r^2 \cdot v^3 \cdot t$$

Eq. 4-3

From that we can easily find the actual wind power for any time instance:

$$P_{wind} = \frac{1}{2} \cdot \rho \cdot \pi \cdot r^2 \cdot v^3$$

Eq. 4-4

Finally, the dominating parameter for wind power is wind speed, as it counts with the power of 3 into the calculation. It is also much depending on the crossed area and to a certain amount on the air density.

4.3.2 Rotor Theory

As the electric generators are usually rotating machines (linear generators are existent as well) we need to transform the almost linear power flow into rotational power flow. A well known principle to accomplish that task can be found from aircraft engineering. Long before commercial wind turbines[1] were developed, engineers found a way to change force directions by the help of wings and the ascending principle[2].

A restrained wing that is blown by a wind stream will create forces. Because of the specific wing profile there exist different wind speeds at the upper and lower surface. These give a pressure unbalance causing an ascending force which we call lift force F_{Lift}. The projected area towards the wind will additionally raise a thrust force F_{Thrust}. The addition of lift and thrust force vectors forms a first torque force F_{Torque} that will turn the rotor from rest.

As we have the rotor blades spinning, we can imagine that there will be a virtual wind blowing towards the upper blade surface. Together with the true wind the blade will see its own wind. Thus, it is necessary to adjust the blade angle to reach the optimal lift force. This angle is referenced to the corda line of the profile and also called angle of attack β_{pp}.

---

[1] First wind turbine was built by Charles F. Brush, Cleveland, Ohio – the turbine had 144 rotor blades made of cedar wood and was 17 meters tall. It was operated by the resistive principle.

[2] In the 1920s, the German physicist Albert Betz published first studies about optimal aerodynamic form giving of wind turbine blades. He showed that a turbine running by the ascendant principle can be more efficient than one running by resistive principle.

If the corda line and the resulting wind vector are aligned the angle of attack is zero and we have the optimum blade position to create the maximum lift force for one wind speed value. Suddenly it is clear, that for optimal aerodynamic conversion we need to adjust the rotor speed according to the present wind speed, otherwise we do not obtain optimal conditions for the aerodynamic profile.

Due to different rotational speeds along the wing the designed blade profile will never look uniform.

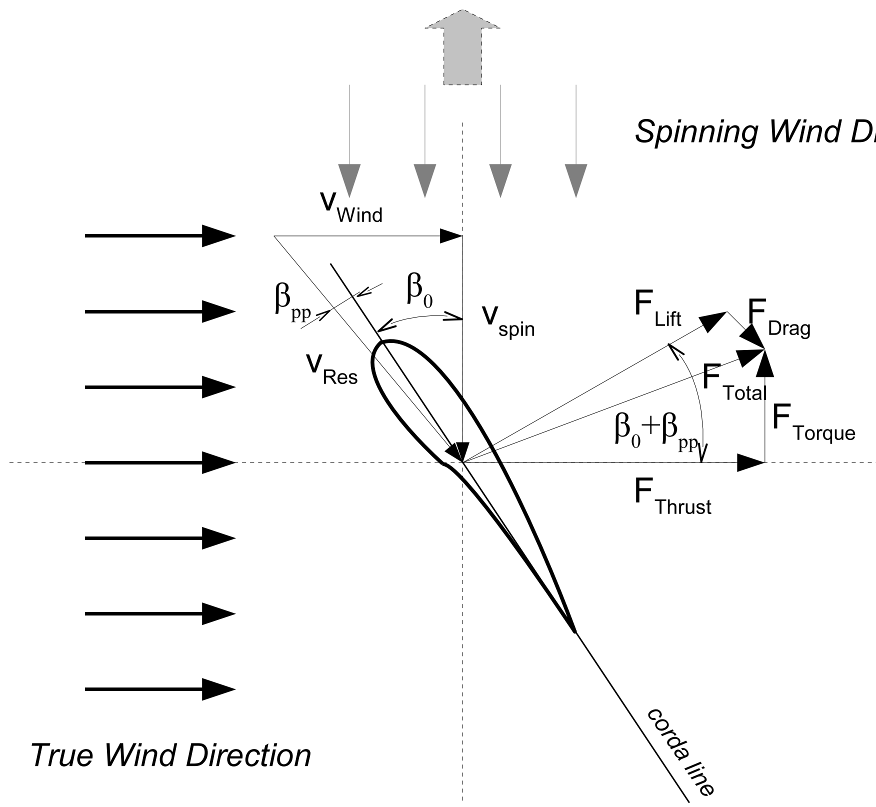

Figure 4.3-1 Example-construction for the torque creating force by one blade (pitched state)

In the picture above β_{pp} is the angle of attack and shows a slightly pitched-out blade. This indicates that a pitch mechanism is already working.
At higher speeds the resulting torque force is also reduced by a dragging force.

Finally, the adjustable angle β_{pp} makes it possible to lower the torque force by pitching the blade out of the optimum. By that mechanism, the maximum power to the generator can be limited.

Regarding the available power in the wind, the question occurs how effectively power can be taken out of it.

When power is taken out by the blades, the rotational speed of the rotor slows down. We can imagine that it is not reasonable letting the rotor come to rest. This would mean we do not take out any power out of the wind. The German Albert Betz was facing the problem also, and in 1919 he published a solution for disc like rotors – the Betz' Law. He tried to express the action of wind braking in an equation. By putting the wind speed far in front of the turbine into the right relation to the wind speed behind the turbine, he found the equation for the so called *power coefficient (C_p)*. The power coefficient is defined as following:

$$\frac{P_{Turb}}{P_{Wind}} = C_p$$

Eq. 4-5

We already derived the power in the wind:

$$P_{wind} = \frac{1}{2} \cdot \rho \cdot \pi \cdot r^2 \cdot v^3$$

Eq. 4-6

Putting Eq. 4-6 into Eq. 4-6 we find the generally used formula for calculating the power of a wind turbine:

$$P_{Turb} = P_{Wind} \cdot C_p = \frac{1}{2} \cdot \rho \cdot \pi \cdot r^2 \cdot v^3 \cdot C_p$$

Eq. 4-7

The power coefficient according to Betz[1] is:

$$C_p = \frac{1}{2} \cdot \left(1 + \frac{v_2}{v_1}\right) \cdot \left(1 - \left(\frac{v_2}{v_1}\right)^2\right)$$

Eq. 4-8

where: v_1 is wind speed in front of the rotor
v_2 is wind speed behind the rotor

Actually, C_p indicates how much power we can take out of the wind by giving an equivalent braking. C_p does not show how this breaking is achieved. But, the formula for C_p can show at least the theoretical maximum. This maximum is located between two scenarios. If we would take out all kinetic energy by our wind turbine the particle flow would almost come to standstill, air would accumulate in front and further particles would avoid and pass by the turbine. No braking of the particle flow means we will not take out any energy and the power would be zero.

For solving the equation we introduce a braking action without units:

$$x = \frac{v_2}{v_1}$$

Eq. 4-9

We put Eq. 4-9 in Eq. 4-8:

$$C_p = \frac{1}{2} \cdot (1 + x) \cdot (1 - x^2)$$

Eq. 4-10

Solving this equation for the maximum, with $x = \frac{1}{3}$:

$$C_{p\_\max} = \frac{16}{27} \approx 0.593$$

Eq. 4-11

[1] Proven in *Albert Betz, Windenergie und ihre Ausnutzung durch Windmühlen, 1926*

This means, the highest possible power we can theoretically get out of the wind power is 59.3%. Therefore the wind will be broken down to 1/3 of its original speed.

Unfortunately, for wind turbines C_p is not constant. The most common parameters for C_p are the tip speed ratio λ and the pitch angle β.

$$\lambda = \frac{TipSpeed}{WindSpeed} = \frac{\omega_r \cdot r}{v}$$

Eq. 4-12

The power coefficient $C_p(\lambda, \beta)$ is a function of both parameters. Explanations for that were already given in the abstract about the creation of the force vectors. Consequently different wind speeds call for optimal tip speed and pitch angle to achieve a high C_p and therefore giving the highest power output.

In fact, blade losses are by far the biggest absolute losses in wind turbines, therefore high power coefficients are important. Modern built rotors achieve maximum power coefficients of C_p= 0.48...0.54[1] so the blade losses can become 10 to 22 percent

The mentioned aspects make very clear - to get maximum power out of the wind we need to have a wind turbine that allows changing the rotor speed to reach optimal aerodynamic conditions. As C_p has a maximum for one λ we have to control our tip-speed according to the wind-speed to always reach the optimal λ the blades are designed for. This task will be called Power Point Tracking (PPT)

[1] C_p from Enercon E-82 wind turbine

4.3.3 Turbine Operation States

If we face just any strength of wind to a turbine we will have to consider two things. First, there will be friction in the mechanical systems that we have to overcome giving a certain cut in speed where the turbine will start to spin. Second, the power of the generator is limited. Therefore we should have a limit in rotor speed to prevent overload mode.

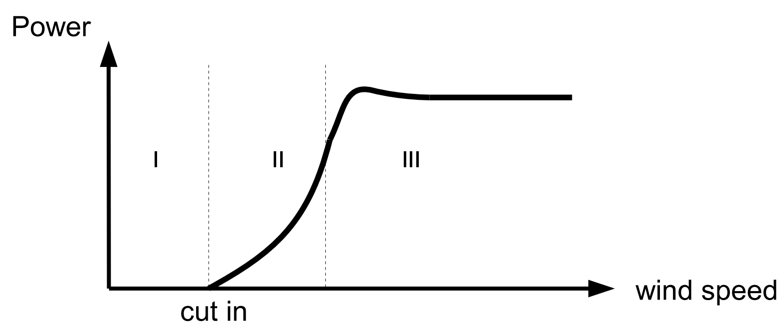

Figure 4.3-2 Powercurve and operation states of the passive pitched wind turbine

Figure 4.1-1 shows the basic operational states including the cut-in point where the rotor starts to spin and can be described as following:

I. **Standstill**, the turbine is not spinning due to friction in the bearings.

II. **Normal Operation**, starting at cut-in wind speed the turbine follows the power curve if the regulation works properly.

III. **Pitched Operation**, the power is limited by reducing the angle of attack. Actually, the beginning cannot be defined at one specific wind speed as even short wind gusts activate the pitching mechanism.

4.3.4 Real Rotor Parameters

This sub-chapter will look on the parameters for the 30 kW Pitchwind rotor. To do good Power Point Tracking, it needs to have precise aerodynamic parameters from the rotor. Otherwise it is not possible to calculate the correct power we would like to take out and operate the turbine at wrong operation points with low efficiency.
Therefore we introduce optimal parameters for our rotor where:

$$C_{p,optimal} = optimal\ \ power\ coefficient$$

$$\lambda_{optimal} = optimal\ \ lambda$$

Both refer to each other - $C_{p,optimal}$ therefore is reached at $\lambda_{optimal}$.

Unfortunately, these values are not precisely given any more. Up to know there have been "believed" parameters for optimal turbine efficiency. To overcome this lag of information we need to find a way to get acceptable values.
The only way to access these parameters was found in back calculation of old measurements taken by the Swedish FFA[1]. The measurements were taken for power performance evaluation of the wind turbine. The complete title of the report can be found in [22]. Only real life measurements with a lot of taken samples sorted in specific bins are usable to find the operational points of a wind turbine. As for these measurements there had been another setup of power electronics we have to take that into account for a back calculation.

The C_p over wind-speed curve has been created by use of *Figure 5* of the report [22] and is presented in *Appendix B*. As only the electrical power coefficient is provided, we have to back calculate with assumed efficiencies for all the power electronic components installed at that time as well as the generators efficiency. The values assumed can be found in *Appendix B*. The λ over wind-speed curve is derived from *Figure 7* of the report [22] and given in *Appendix B*.

---

[1] FFA – Flygtekniska Försöksanstalten, The Aeronautical Research Institute of Sweden

Finally, the following chart has been derived from calculations in the Excel sheet "*Cp_curve_oldsystem.xls*":

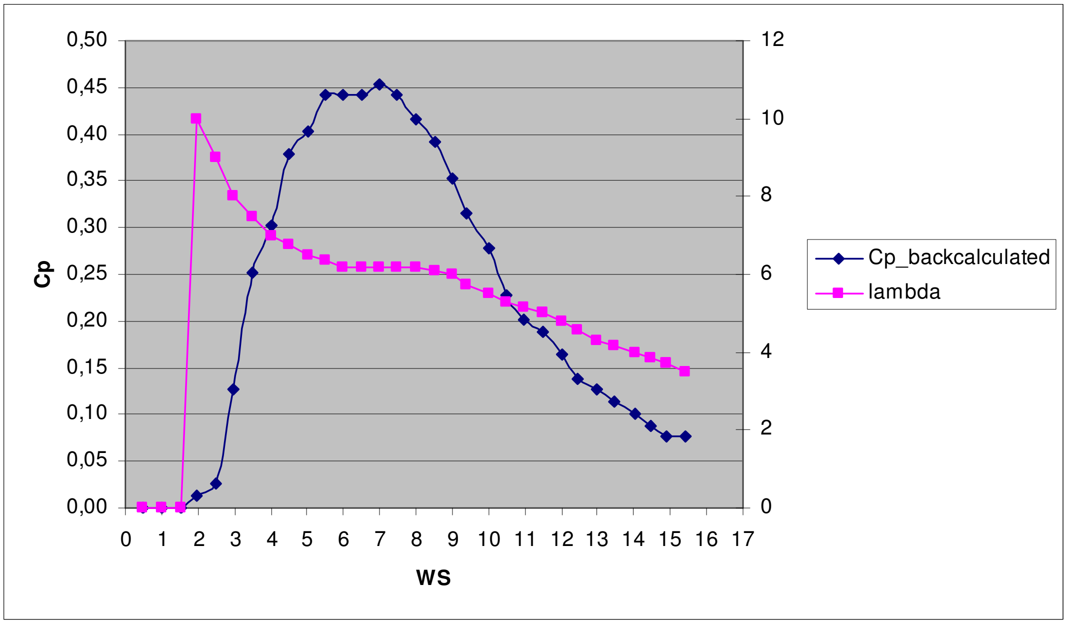

Figure 4.3-3 Back calculated Cp over wind-speed and λ over wind-speed curves from an older power evaluation performed by the FFA.

Looking at the curves we can find the values for $C_{p,optimal}$ and $\lambda_{optimal}$:

$$C_{p,optimal} = 0.45$$

$$\lambda_{optimal} = 6.3$$

The value of $C_{p,optimal}$ seems to be realistic if we compare it to other $C_{p,optimal}$ values of systems similar in rotor size[26].

If we compare these new values with the "believed" ones we get the following result:

	optimal lambda	resulting Cp	relat. to 100%
back-calculated values	6,3	**0,45**	100%
believed values	7	**0,32**	71,11%

Table 4.3-1 Comparison of back-calculated and "believed" values

The comparison shows, that actually the current PPT control might not operate the turbine in highest aerodynamic efficiencies. With operating at the “believed” value for lambda, we only achieve 71 % of the maximum possible power output. One can imagine how this does effect the annual energy production of the wind turbine.

4.3.5 Mechanical Rotor Design

For this turbine the pitch mechanism is passively implemented. The blade consists of a fixed part and a part that can be turned and perform the pitching. The pitch mechanism is called “passive feathered pitch” and realized by torsion springs inside the blades, therefore the thrusting air will adjust the right angle of attack to prevent overspeed and overpower condition.

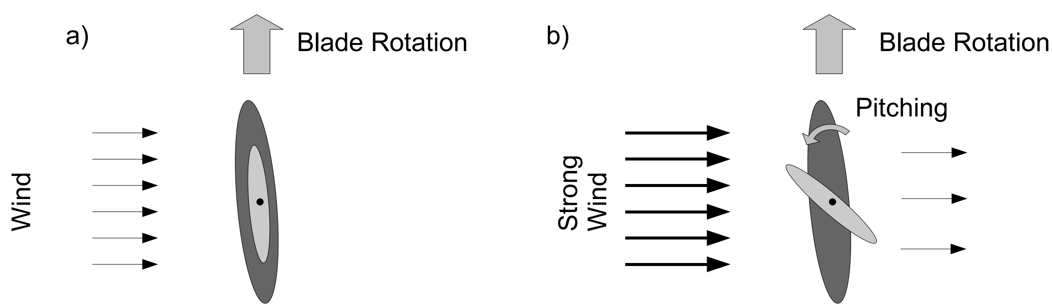

Figure 4.3-4 Principle of pitch operation a) low wind, no pitching b) strong wind or wind gust making outer wing to pitch out

A big advantage of the feathered pitching method is the very dynamic response to strong wind gusts. Other systems applying centrifugal pitching are not able to pitch out very short fluctuations and send higher stress towards the shaft and the tower.

As the blades are made mainly of steel and little fibreglass cloth, the high mass increases inertia and therefore makes it ideal to store energy for short dips in wind speed.

Some problems occur for the applied two-blade design. The idea of taking two blades instead of three is to save costs and reduce complexity. But in practice the two-blade design shows also drawbacks that tend to excite the turbine/tower more. As explanations of all mechanical phenomena on turbine rotors are rather complex and most of them can be found in the literature, only a short comparison is given:

	Two Blade Design	Three Blade Design
speed	faster	slower
noise	louder	more quiet
construction	flapping hub	rigid hub
cyclic gravity load	yes	no
distribution of wind load	uneven	more even
cost	cheap	more expensive

Table 4.3-2 Comparison of Two-Blade and Three-Blade Design

It is obvious that there will be more frequently varying forces towards the nacelle and tower in the two-blade design. The additional mechanical stress will reduce lifetime of components or may call for more maintenance. As the system experiences a stronger resonance at approximately 38 rpm it is recommended to operate above this rotor-speed.

To further reduce stress from the rotor towards the nacelle and the tower a flapping hub is used. A second reason to apply a flapping hub is to avoid problems with the passive feathered pitch mechanism where high friction in the pitch-bearings during high wind loads would prevent the outer wing from pitching. To overcome this difficulty, a flapping hub is used.

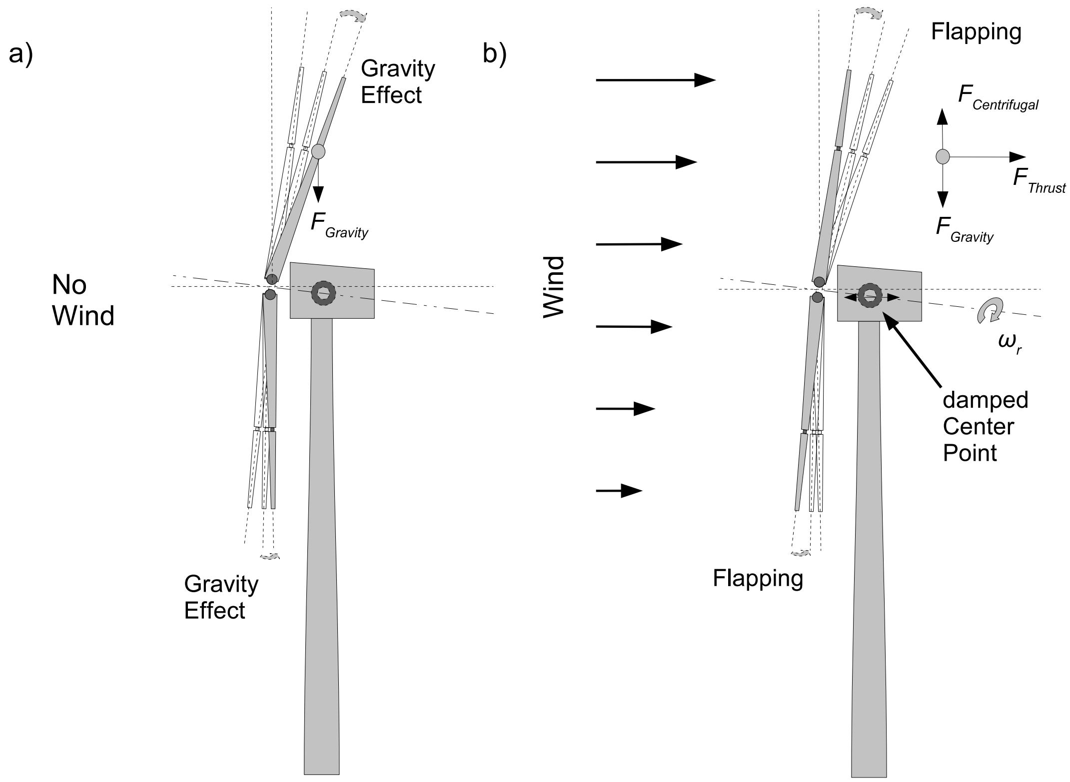

Figure 4.3-5 Principal of a flapping hub for a two-blade turbine a) at rest, b) spinning

Main feature of this flapping hub is to keep the turbine close to the central static point as the bending blade will shortly take out the force of the wind. The flapping hub is able to equal out strong wind gusts very effectively, by that mechanical excitations are damped which is also called *"Aerodynamic Damping"*. This feature makes the turbine very easy to set up on different local towers as tower stress and resonances are effectively reduced. A drawback of this method is considerable deterioration of the blade bearings. Strong, frequently changing forces cause high stress in the flapping joints.

4.3.6 Turbine Classification

After knowing the basic principles the turbine can be classified.

The used wind turbine is operated in variable-speed mode. Thus, a specific wind-speed always leads to a corresponding turbine-speed. The turbine uses passively pitched rotor blades to limit power. Therefore, the system is called variable-speed, pitched controlled wind turbine.

Due to the horizontal rotational axis, the wind turbine belongs to the HAWT (Horizontal Axis Wind Turbines) class[1].

As the rotor-shaft is directly connected to the generator without any transmission gear in between, we can also classify the system into direct driven wind turbines.

One more specific detail is the flapping hub – in contrast, big turbines usually apply rigid hubs.

4.4 Generator

In principle the generator is a machine that relies on the basic phenomena of magnetic fields and electric fields. The Danish chemist Hans Christian Ørsted discovered the relation between electricity and magnetism the so called electro-magnetism in 1820.

$$E(t) = -\frac{d\Phi}{dt}$$

Eq. 4-13

By changing a magnetic field, an electric field can be created, respectively changing an electric field can create a magnetic field.

As it was possible to create magnetic fields - the interaction to other magnetic fields could achieve mechanical motion. Proven by Hendrik Antoon Lorentz, electric charges that travel through a magnetic field do cause forces. The equation of the magnetic component shows how the force is being generated:

$$dF = \frac{\partial q}{\partial t} \cdot (dl \times B)$$

Eq. 4-14

[1] Vertical Axis Wind Turbines (VAWT) are also existent

Regarding the travelling charges as a current:

$$dF = I(dl \times B)$$

Eq. 4-15

Put together, the phenomena of Lorentz and Ørsted finally lead to the idea of an electric machine that was able to convert mechanical power into electrical power by the help of magnetism. Regarding the equations, it is important to know, that a continuous power conversion can merely be done by use of alternating current.

Over the years scientists discovered the amazing opportunities given by this principle. Both applications - motor and generator were investigated. Finally, 46 years later the breakthrough in generating electricity was made by the German Werner von Siemens by developing the “Dynamomaschine” –an electric machine applying the rotational machine geometry.

4.4.1 Generator Type

When it comes to wind turbines, an exciting task is to design the right drive-train and within that, a suitable generator. The turbines generator has two major tasks. First, it is supposed to recover electrical energy – second, by adjusting the electrical load the generators braking torque will control the speed of the turbine to achieve the optimal tip speed ratio λ for a high C_p at present wind speed. The current system is supposed not to use any gear[1], and will be operated in variable-speed mode. Therefore a generator for low speeds (20-75 rpm) and very high torques has to be used.

To get an image of the desired load torque a quick calculation can be done:

$$T = \frac{P}{\omega}$$

Eq. 4-16

[1] A discussion about direct driven generators in wind application can be found in [31]

Supposed to have 30kW mechanical Power and 75 rpm rated speed:

$$T = \frac{30kW}{2 \cdot \pi \cdot 1{,}25 \cdot s^{-1}} \approx 3820Nm$$

Eq. 4-17

In comparison, usual vehicle combustion engines of 30kW power size produce nominal shaft torques around 95 Nm at 3000 rpm speed. Thus, for this example the torque the generator has to deal with is around 40 times higher.

First we will look on a general equation [32] describing the specific power out of an electrical machine. This helps to see which quantities contribute to the power production.

$$P = T \cdot \omega = \frac{\pi}{2} \cdot (\vec{B} \cdot \vec{A}) \cdot d^2 \cdot l \cdot \omega$$

Eq. 4-18

The torque is mainly determined by the magnetic flux density *B*, the electric loading *A*, the machine diameter *d* and the active length *l*. In conclusion a generator with high specific torque requires high magnetic flux density, high currents and rather big dimensions.

One aspect sometimes overlooked is the maximum torque ripple. As we are not going for super-precise servo control one might ask why that is important. In fact, regarding the high nominal torque - only 5% torque ripple and a large rotor could result in a high oscillating mass which could cause damage to the mechanical construction, especially if resonance frequencies are touched. As we are at low speed, the most affecting ripple is the cogging torque.

Another requirement of wind turbine generators is high efficiency across a wide speed range. As variable speed turbines operate in different speed regions it is important to assure good efficiencies to get most power at any operation state.

Last but not least, to reduce tower stress, production cost and shipping cost the generator should have a good torque to weight ratio.

After knowing some aspects the main requirements can be taken down as following:

- High torque ability
- Low cogging torque
- High torque/weight ratio
- High efficiency over wide speed and load range

One topology that suits to these requirements might be the permanent magnet synchronous machine (PMSM)[1] in combination with a frequency converter.

Usually, the design process for a specific generator is most comprehensive and takes a lot of time and understanding. To describe, why a generator is designed in that way and no other might become rather complex. Many issues like electrical, mechanical and thermal parameters are referring to each other. Therefore only some important reasons for a PMSM design are presented here:

I. **Permanent Magnets**, since the use of permanent magnets eliminates the need for windings on the rotor the resistive losses are approximately half. They also allow a smaller pole pitch (see II.) and reduce weight as a winding would weigh much more [31].

II. **Small Pole Pitch,** allows the stator yoke and rotor yoke to be made thinner, by that the generator becomes lighter. But also the amount of inactive copper in the end windings can be reduced [31].

Still, there are some options on how to design the right PMSM. One could decide to go for an air gap winding. By that, cogging torque could be avoided because there are no teeth. But, all of the generators torque will be put by half on the air gap winding. This would need a very stable winding construction that withstands strong torsion stress. Also, the surface to conduct heat to the environment would be reduced and there will be more thermal resistances to be overcome. For that reason, a machine using back iron seems reasonable.

Finally, there is the option to built radial or axial flux machines. Even most of the literature does not give clear answers here. The most industrial machines are by far radial

[1] PMSM generators are also applied at 1.5MW systems of Vensys GmbH & Co. KG, Germany

flux machines. Regarding the application of radial flux machines it can be figured out, that the most common applications are those that have to consider narrow dimensioning specifications. In concrete terms, if the length of the machine is much limited the axial flux topology might be preferred even if two machines are stacked together[1].
As this application does not have special demands for a short length the radial flux design retains a good choice.

As the wind turbine will only experience low speeds, surface mounted magnets are a good choice because the effective air gap is being kept small and the risk of ripping magnets of is low. Also the assembly of the rotor can be simplified.

Most important for good wind generators is a robust design. These generators are facing high mechanical stress but also experience rough climate conditions. Therefore it needs to take some actions during the assembly. One important aspect is the mounting of the magnets and the sealing of endangered components (e.g. winding, bearings, and magnets). For mounting the magnets very robust and long durable glue should be used that also can withstand the specified temperature band. Further there needs to be a careful sealing of the winding and the magnets, this is to protect from corrosion. In case the magnets start to corrode, the magnet surface material will transform to oxide and remain as powder without any chance to remain at the original position.

4.4.2 Generator Parameters

First, the stator resistance R_s is being measured by opening the star connected phases and putting 5 Amperes through one phase and measuring the voltage drop over the phase.

$$R_s = \frac{U}{I} = 0.368\,\Omega$$

Eq. 4-19

[1] The axial flux design allows for various design combinations of rotor and stator

The inductance L can be isolated out of the phase-impedance:

$$Z = \sqrt{R_s^{\ 2} + (j\omega L)^2}$$

Eq. 4-20

solved for L

$$L = \frac{\sqrt{Z^2 - R_s^{\ 2}}}{\omega}$$

Eq. 4-21

Z can be determined by measuring the open-circuit voltage and short-circuit current at rather low speed:

$$Z = \frac{U_{OC}}{I_{SC}} = \frac{16.77V}{43.14A} = 0.3887\ \Omega$$

Eq. 4-22

the electrical frequency is:

$$f_{el} = p \cdot f_{mech} = 3.13\,Hz$$

Eq. 4-23

Now, the inductance can be calculated:

$$L = \frac{\sqrt{Z^2 - R_s^{\ 2}}}{2\pi f_{el}} = 6.36\ mH$$

Eq. 4-24

It is interesting to see if the AR who actually determines the values automatically will use similar values. Therefore a comparison table is made.

	Measured	AR (auto)
Rs (mOhm)	388,7	384,5
Ls (mH)	6,36	5,16

Table 4.4-1 Comparison of Measured and AR determined generator parameters

The values match good for the stator resistance, the difference of the stator inductance could be caused by a different measurement method and different measure-currents.

4.5 Active Rectifier and Grid Inverter

Basically, the Active Rectifier (AR) and the Grid Inverter (INV) are three phase power inverters. Three phase inverters are widely used to supply three phase loads, typical applications are ac power supplies, grid-coupled inverters, island-grid inverters and motor drives. In this application the employed AR is a motor drive in regenerative mode and is supposed to be a IGBT-6-pulse voltage-source inverter. The second inverter is used to establish a local grid and is also of IGBT-6-pulse type. This combination of two three-phase inverters with an intermediate DC-link is very often named “back-to-back”-inverter.

Inverters are switched mode converters that transform from direct current (dc) to alternating current (ac) bidirectional. The operation modes of switched mode converters can be described by showing the active quadrants. Assuming the inverter load on a single phase to be a motor/generator, we can imagine connecting a simple inductance instead. This leads to a phase lag between voltage and current in this simple circuit. To fully control this circuit the converter needs to be able to operate in all four quadrants of the voltage-current plane.

In practice, three phase four-quadrant inverters are built by three separate switching legs and look like in the figure below.

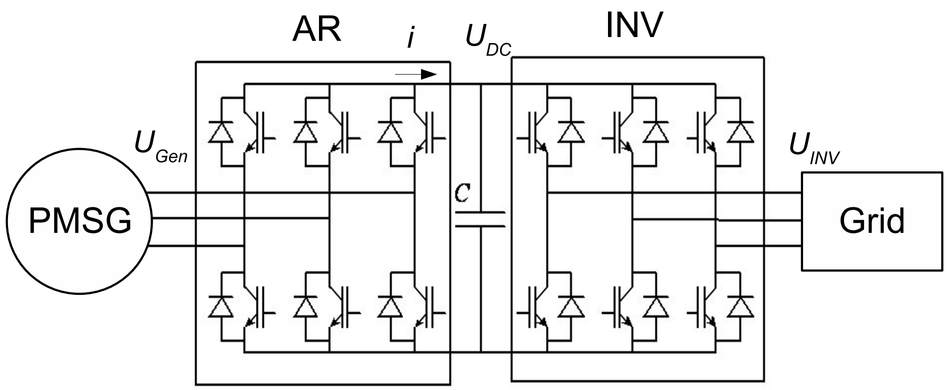

Figure 4.5-1 Two three phase 6-pulse inverters in "back-to-back" configuration

The system application gives the following voltage specifications to these Inverters

- U_{Gen} = 140 V to 400 V
- U_{DC} = controlled voltage, adjustable between 550 VDC and 650 VDC, can drop to battery level of approximately 420 VDC under load
- U_{Grid} = 400 V (rms)

U_{DC} will be determined by how much the DC-Link capacitor will be charged. Due to the controlled voltage source behaviour of the AR it is always possible to take out some current by adjusting its output voltage to lower values than the generator phase voltage U_{Gen}. The voltage over the capacitor can be described by:

$$U_{DC} = C \cdot \int (i_{DC})dt$$

Eq. 4-25

In case there is not enough power to supply the necessary current to stabilize U_{DC} the voltage will drop to the battery voltage. At that point the INV will see the battery as a voltage source but having only about 430 VDC on the DC-Link.

As it is not precisely known in which mode the inverter is being operated it could be assumed that it operates in linear regions where the relation for U_{DC} and U_{INV} is given as [28]:

$$U_{INV(RMS)} = \frac{\sqrt{3}}{2\sqrt{2}} \cdot m_a \cdot U_{DC}$$

Eq. 4-26

where: m_a is the modulation index if PWM-Modulation is applied

The maximum sinusoidal phase voltage can be reached if over-modulation is applied. This will force the inverter to go into square-wave operation where U_{Gen} is given as [28]:

$$U_{INV(RMS)} = \frac{\sqrt{6}}{\pi} \cdot U_{DC} \cong 0.78 U_{DC}$$

Eq. 4-27

Setting the lowest U_{DC} voltage to the battery level:

$$U_{INV(RMS)} = 0.78 \cdot 420V = 327\,V(rms)$$

Eq. 4-28

Obviously the phase voltage calculated in Eq. 4-28 is too low to meet the requirements. Therefore it is necessary to connect an output transformer in the system as well. The transformer therefore needs to have a transmission ratio:

$$\ddot{u} = \frac{N_2}{N_1} = \frac{U_{Grid}}{U_{INV}}$$

Eq. 4-29

By calculating with the specified values we find:

$$\ddot{u} = \frac{400V}{327V} \approx 1.22$$

Eq. 4-30

In case the INV is not operated in square-wave operation the transformer ratio needs to be higher. To be on the safe side, a transmission ratio of 1.5 or more should be used instead.

A second aspect on using a transformer is the limited ability of the INV to deliver high currents to blow safety fuses included in further infrastructure. The stored energy in a transformer will accomplish this task and also provides galvanic isolation which in some cases is needed. Even though, simple hybrid power systems that just run a pump or similar simple applications can be operated without a transformer.

4.6 Reactive Compensation

If direct driven PMSGs are designed for wind application they will usually have high inductances simply by having many windings in the stator. Common ranges for stator inductance values are 5 mH to 100 mH [23]. If the speed of the turbine increases and the phase voltages rises there will be quite high voltage drops over the windings which in turn reduce the maximum output power. Usually if big generators are directly connected to the grid, they will obtain reactive power from the grid as long as possible. As we have controlled inverters and an in between DC-Link in our setup this will not be possible at any time. In order to get high power out of the generator we have to supply reactive power for compensation. This can be achieved in three ways:

1. Active Compensation by a controlled four-quadrant converter (Active Rectifier)
2. Passive Compensation by capacitors in parallel to the phases
3. Passive Compensation by capacitors in series to the phases

Investigations from *M. Bartholet* and *C. Zwyssig* [24] show that series compensation has superior behaviour over parallel compensation. Therefore, Option 2 is not taken into account.

Meanwhile compensation is accomplished by an Active Rectifier. The task is to investigate if passive compensation could be an option to reduce cost.

Besides the investigations from *M. Bartholet* and *C. Zwyssig* experiments performed by *J. Linström* [30] showed, that power factors close to one will not achieve the highest efficiency in some electrical machines of PM-type. As this discussion would not fit in the thesis frame it has been left out and should be regarded in a separate work.

4.6.1 Compensation with Active Rectifier

The used active rectifier (AR) actually is a voltage controlled IGBT-6-pulse inverter with so called "Drive"-functionality. More information on how the power factor in a generator is controlled can be found in chapter 4.7.3 where the generator control and the DTC are being discussed

4.6.2 Series Compensation

If series compensation is applied instead of the use of an AR, the setup will change as following:

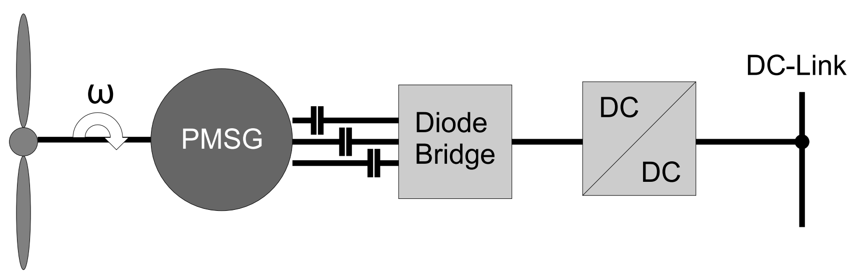

Figure 4.6-1 Setup with Series-Compensation

As can be seen, three new components are introduced. First there are the compensation capacitors in all three phases, followed by a diode-bridge and finally a DC-DC converter for current and voltage control.

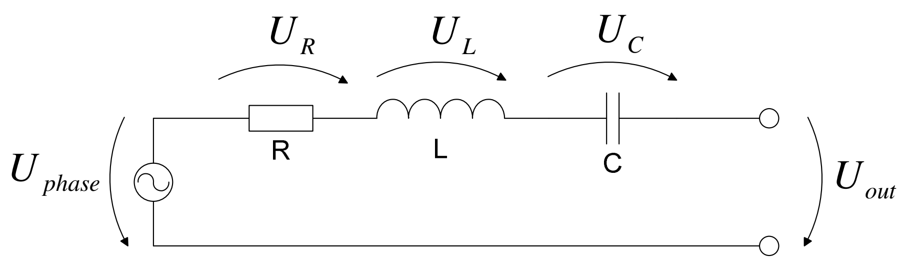

Figure 4.6-2 Series compensation circuit for one phase where C is the compensation capacitor

As the need of reactive power for the generator is proportional to the current it will be supplied by capacitor C. If the capacitor is calculated for rated power at rated speed it will provide just enough reactive power to completely compensate. Obviously, if the generator turns slower and the voltage U_{phase} decreases, the capacity for C drops as well. That means the compensation will be not so effective for lower speeds. As the power at low speeds actually is very low - the effect of not having complete compensation has not such a big impact.
Finally, series compensation has the advantage of not increasing the terminal voltage for open-circuit or low load condition which actually limits the amount of compensation when parallel capacitors are used. Series compensation is not load dependent but dependent on the generators speed.

For a better understanding it is possible to draw the behaviour of currents and voltages in a phasor diagram:

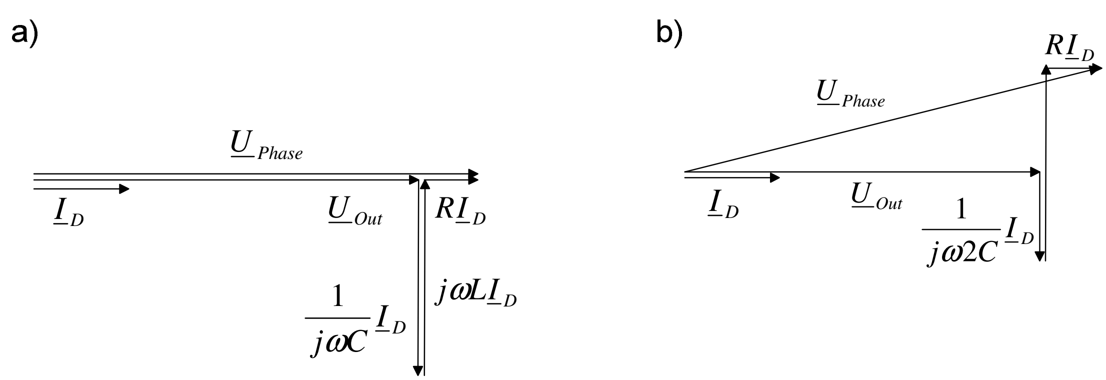

Figure 4.6-3 Phasor diagram for series compensation a) full compensation b) half compensation

In Figure 4.6-3 we can now see what happens with the generated voltage $\underline{U}_{Phase}$. If we compensate completely only the copper losses reduce $\underline{U}_{Phase}$ down to $\underline{U}_{Out}$. The output voltage $\underline{U}_{out}$ will be more reduced if we do not compensate completely. The phasor diagram clearly shows a phase angle between U_{Phase} and U_{Out}.

The capacitance C for full compensation will be calculated as following:

The impedance in the circuit is:

$$Z = R + j\omega L + \frac{1}{j\omega C}$$

Eq. 4-31

Full compensation implies:

$$j\omega L + \frac{1}{j\omega C} = 0$$

Eq. 4-32

According to Eq. 4-32 we can calculate:

$$C_{full} = \frac{1}{\omega_{rated}{}^{2} \cdot L} = 1.96\,mF$$

Eq. 4-33

where

$L = 6.36\,mH$	Inductance of one generator phase
$\omega_{rated} = \frac{2\pi}{60}\,pn_{rated}$	Rated electric angular frequency
$n_{rated} = 82\,rpm$	Rated rotor frequency
$p = 33$	Number of pole-pairs

The value calculated is quite high and three capacitors of that size are needed. For a complete turbine control, a diode-rectifier and a DC/DC-converter are still needed. The diode-rectifier can be of ordinary six-pulse type with adequate rating. Also we have to make a choice for a suitable DC/DC-converter. Regarding in- and output-voltages we have to select a suitable converter-topology. Basically this application will need a step-up converter. Usually boost-converters are employed as they indicate a good switch utilization in this type of application [25]. As no further design criteria have to be met, the boost converter would be favoured.

4.6.3 Comparison of Compensation Methods

To compare the active compensation against the passive series compensation two aspects are regarded:

- Performance of the compensation method
- Cost of the compensation method

First the performance of both methods is compared. Therefore the turbine operation range is divided into three regions and the compensation performance is weighted. Sources for power factor measurements of the AR setup can be found in *Appendix B.* Values for the power factor for the series compensation are taken from [25].

Power-Level	Compensation by Series-Method	Compensation by Active-Rectifier
low	poor	average
medium	very good	very good
high	very good	very good

Table 4.6-1 Comparison of the compensation performance for different speed-regions

Regarding the performance, both methods come close to the same results, only for lower power-levels an actively controlled rectifier performs better.

Another issue is the cost of both solutions. After doing some research it seems cost intensive to do a certified and tested solution for the series-compensation electronics. Compared to the almost very moderate cost for the already used AR, it seems that the AR remains a very good choice.

4.7 Turbine Control

There are three main control issues for the Turbine Control:

1. DC-Link Voltage Control (UDC-Control) *see Chapter 4.7.1*
2. Power Point Tracking (PPT) *see Chapter 4.7.2*
3. Generator Control (DTC, sensorless) *see Chapter 4.7.3*

As option, it should be found out if battery charging is possible by the DC-Link itself:

4. Battery Charge Control *see Chapter 4.7.4*

As stated in Chapter 4.1 some major components of the system change. The following figure shows, in which way the turbine control was done in the old system:

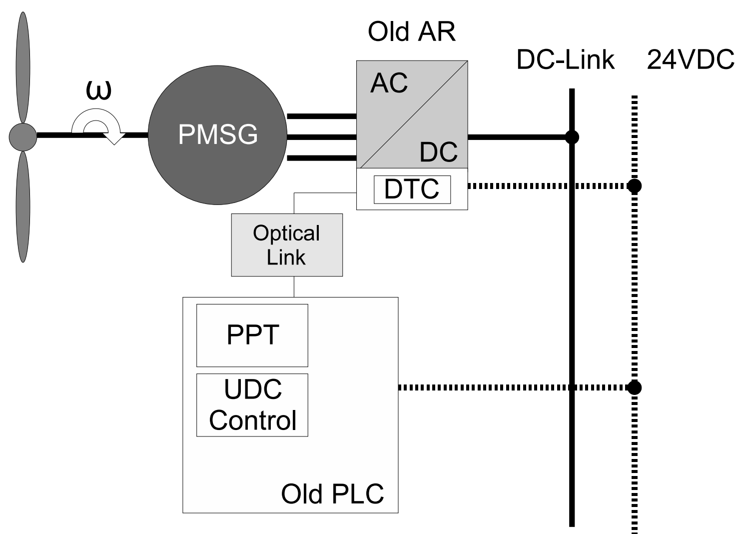

Figure 4.7-1 Old Turbine Control with old control loops and fiber-optical communication

Due to a new AR and a new PLC it has been found out, that some control tasks could be transferred from the PLC to the new AR (see Figure 4.7-2). As cycle-times for calculations in the AR are 10 times faster than external control - a better control performance could be achieved. A free space for own programs at the AR's DSP-based hardware platform seems to allow to run the PPT and UDC-Control inside the AR.

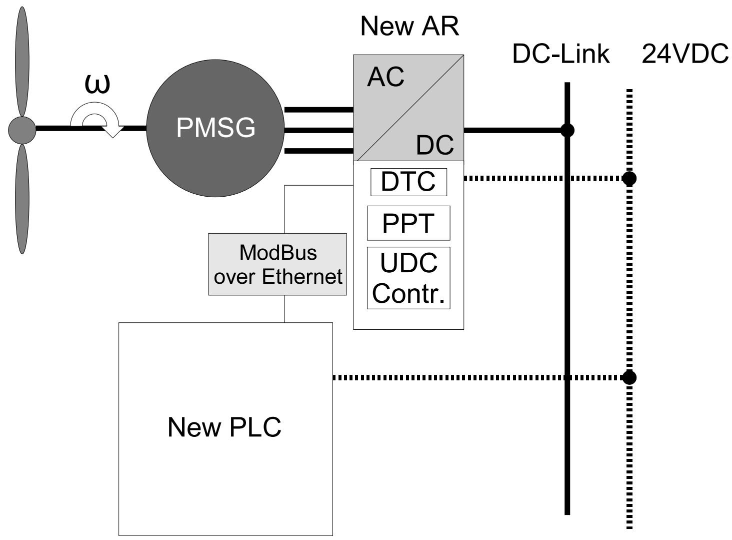

Figure 4.7-2 New Turbine control with Ethernet communication and moved control

The following sub-chapters describe how the PPT- and UDC-loop are being implemented at the onboard-hardware of the new AR.

Further on, the communication between the PLC and AR will be achieved by an Ethernet cable. All the commands coming from the overriding HPS-control are communicated via ModBus over Ethernet.

4.7.1 DC-Link Voltage Control including Multi-Turbine Operation

DC-Link voltage control is necessary to provide a stable DC-voltage to the connected grid-inverter. As soon as the INV is externally loaded, the intermediated DC-Link will be loaded as well. A too low DC-Link voltage would let the INV trip immediately. In this application different types and sizes of INV will be connected to the DC-Link – the correct level of UDC for proper operation should be always present. Common DC-Link voltages for these power systems are 450 to 650 VDC.

Further, the optional parallel operation of two or more turbines demands for a dedicated control of each turbine towards the common DC-Link otherwise the power contribution of each turbine to the DC-Link will be out of control.

Another application where DC-Link voltage control could be employed is to directly charge connected batteries. Some more information can be found in chapter 4.7.4 where this application is described more in detail.

The most challenging requirements are due to multiple turbines running on one DC-Link. A strategy to share the load between them is to program a load line for each of them. The principle of a load line is illustrated below:

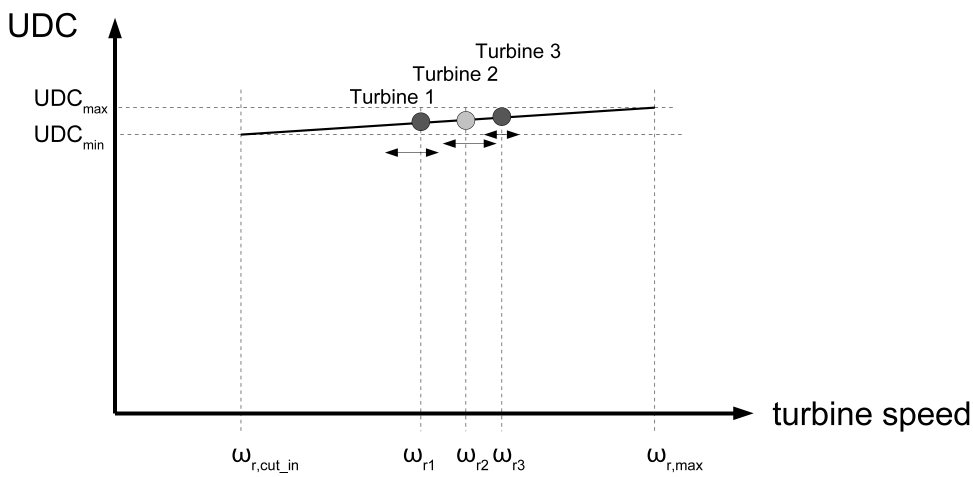

4.7-3 Example for three turbines having operating on the same programmed load line

As seen in the figure above, the applied principle is rather simple. The power output of each turbine will depend on the turbine speed, therefore it will vary at any instance as the wind speed is never constant. To split the load according the actual power level of each turbine the voltage level needs to be controlled. This assures balanced contribution even if there will be no stable condition as the operation points of each turbine will travel. To achieve this control behaviour, the DC-Link needs to be programmed to a lower limit UDC_{min} and an upper limit UDC_{max} including a very slight slope depending on the turbine speed ω_r. The difference between these two limits is expected to be around 10 Volts and needs to be verified by practical tests.
So far, the Multi-Turbine Control has not been tested in practice but is implemented. Up to the end of the thesis work a fixed value for UDC was used in practical experiments.

For the implementation of the UDC-Control the programmable real time frame in the AR is used. The regulation of UDC will be performed by a standard PI-controller which will be configured until stable operation is reached. As in this case the PI-controller is performed in a digital environment it has to be noted, that the controller output needs to be initialized and strictly determined otherwise the intended operation will not be established. Further inputs for the control scheme are the turbine speed and the references as well as the slope to establish the load line. The output of the PI-controller is a secondary torque reference. The reason for that is the limited power and torque by the wind turbine. Therefore the calculated maximum present torque of the PPT-Control needs to be set as a limiting value. The MIN block in the drawing below will avoid torque values above the allowed torque present in the turbine. The final output of the UDC-controller is a torque reference given to the internal torque controller of the AR.

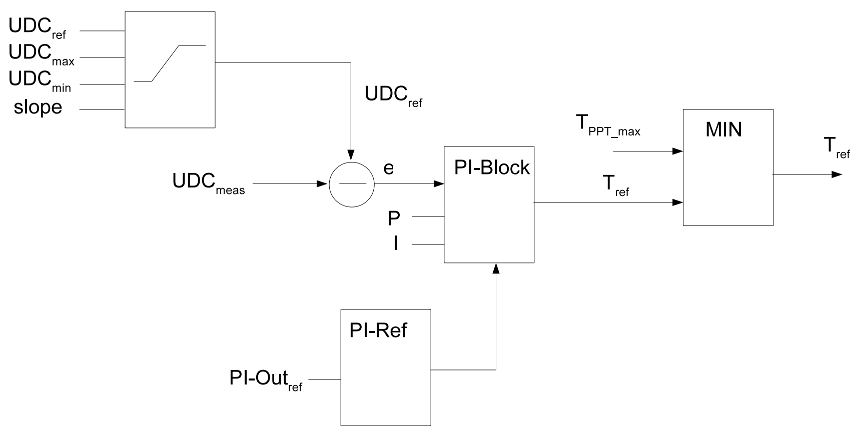

Figure 4.7-4 Simplified UDC-Control implemented in the AR

Not included in the figure above is a programmed very low starting torque which will provide power for the AR itself to start up if no battery is supporting the DC-Link. That can be in times the battery needs to be exchanged. This starting torque will be taken away as soon the AR can track the generator successfully.

4.7.2 Power Point Tracking (PPT)

The next task is to determine how much power we can actually take out of the wind to sustain a stable DC-Link. Although full power is not always needed or provided, we need to know the actual value for maximum present turbine power at any wind-speed *v*. As a control parameter, the power value is translated into a representative torque command.

First, an operation scheme for this special turbine is developed. It will basically comprise the definition of three control regions:

1. **Zero Torque**, the turbine will remain unloaded until the critical resonance speed of 38rpm is securely passed
2. **Linear Torque**, will provide a soft loading towards the Optimal Torque Curve
3. **Optimal Torque** calculates the optimal torque the turbine can be loaded with

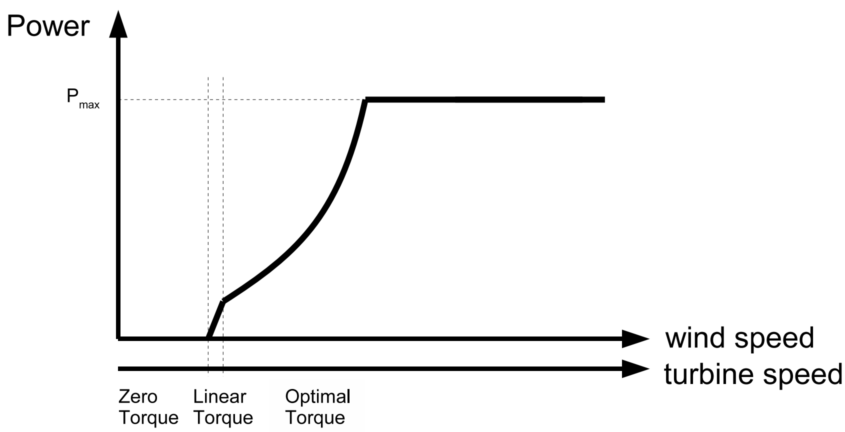

Figure 4.7-5 Turbine control regions

The three control regions will be calculated as follows:

1. **Zero Torque** $T = 0$
2. **Linear Torque** $T = k_1 \cdot \omega_r$
3. **Optimal Torque** $T = k_2 \cdot \omega_r^{\,2}$

The following abstract will explain how Power Point Tracking actually works.

From chapter 4.3.2 we derived the following equation for maximum present turbine power:

$$P_{Turb\_\max} = P_{Wind} \cdot C_{p,optimal} = \frac{1}{2} \cdot \rho \cdot \pi \cdot r^2 \cdot v^3 \cdot C_{p,optimal}$$

Eq. 4-34

To get the maximum power out we need to operate the turbine at $\lambda_{optimal}$.

$$\lambda_{optimal} = \frac{\omega_r \cdot r}{v}$$

Eq. 4-35

This is not so easy. We can measure the rotor speed ω_r but unfortunately we do not know the wind-speed *v*. A*s* we have no anemometer[1] installed that could give us information about actual wind-speed there needs to be another way to calculate the missing value. We could think about using the rotor as anemometer instead.

If we just let the turbine spin and assume to have the right tip speed ratio $\lambda_{optimal}$ we are able to extract the believed wind-speed *v*:

$$v = \frac{\omega_r \cdot r}{\lambda_{optimal}}$$

Eq. 4-36

Having the believed wind-speed value we just keep on calculating the possible turbine power by putting Eq. 4-36 into Eq. 4-34:

$$P_{Turb} = \frac{1}{2} \cdot \rho \cdot \pi \cdot r^2 \cdot C_p \cdot \left(\frac{\omega_r \cdot r}{\lambda_{optimal}} \right)^3$$

Eq. 4-37

We now have calculated the believed turbine power. To take this power out of the generator we need to calculate a braking torque T_{brake} as a command for the AR controllers torque reference:

$$T_{brake} = \frac{P_{Turb}}{\omega_r} = \frac{1}{2} \cdot \rho \cdot \pi \cdot r^2 \cdot C_p \cdot \frac{\omega_r^{\,2} \cdot r^3}{\lambda_{optimal}^{\,3}}$$

Eq. 4-38

---

[1] Anemometers are small instruments measuring the wind-speed

All constants are taken out to form k_2 - by doing this we get:

$$T_{brake} = k_2 \cdot \omega_r^{\ 2}$$

Eq. 4-39

If we now apply the braking torque T_{brake} - what will happen?

We could face three scenarios:

1. **Too much power calculated** and the turbine will immediately slow down
2. **Exactly the right power calculated** and the turbine will keep its speed
3. **Too less power calculated** and the turbine will immediately speed up

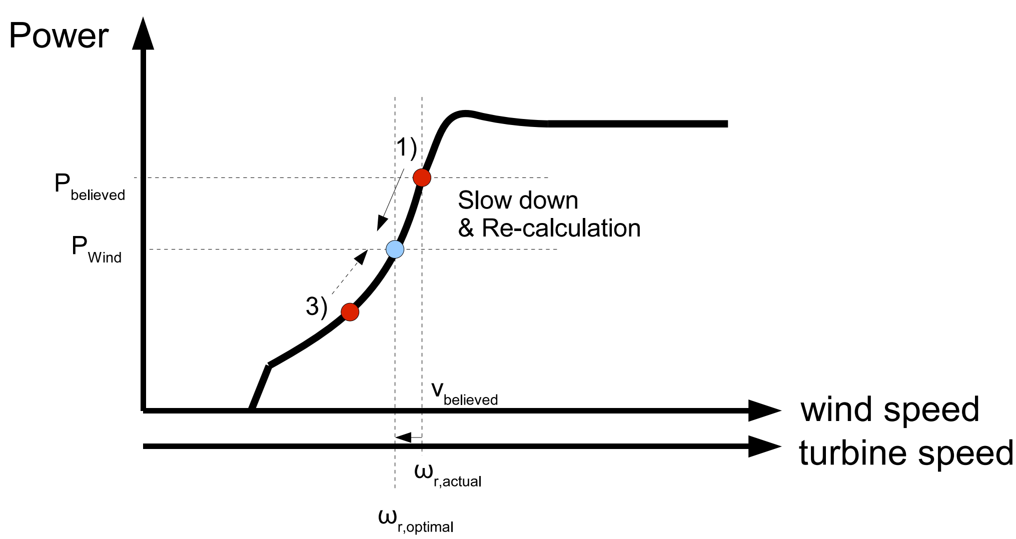

Figure 4.7-6 Principle of Iterative Power control (scenario 1 and 3 are indicated)

According to scenario 2, the turbine speed would be just controlled perfectly. As the real wind-speed is not constant, we will not have that case very often.

If scenario 1 or 3 is true, both are the more realistic scenarios, the turbine speed will change and therefore a new believed braking torque will be calculated. By that, the turbine speed is affected and the turbine will be able to speed up or down depending on if there was stronger or weaker wind. As the PPT calculation runs in a 100ms frame, this will be done quite quickly.

Obviously, the PPT works like a “real-time iteration” that always tries to brake or let go the turbine to reach $\lambda_{optimal}$. The described way shows that turbine control actually remains an issue of torque control. As the former control was implemented as speed control towards zero speed with control of torque-limiting parameters the new control directly calculates a torque reference which further is connected to an internal torque reference for the following DTC (Direct Torque Control).

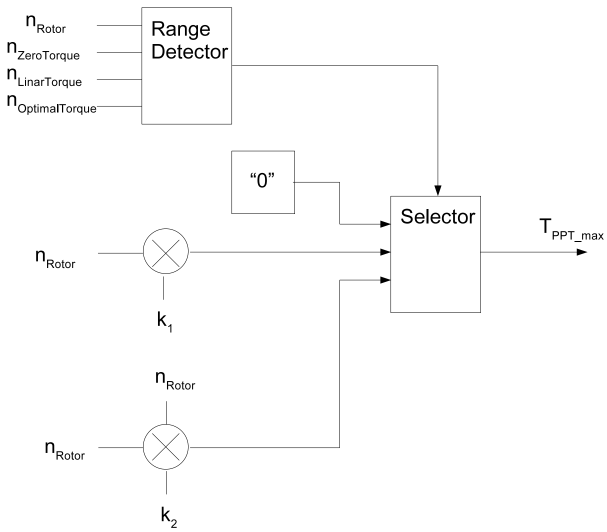

4.7-7 Simplified representation of the implemented PPT-Control

Compared to the former solution, the new PPT-Control will not need any speed controller in between.

4.7.3 Direct Torque Control (DTC)

The task for the DTC is to control both rotor flux Ψ_R and the electromagnetic torque T_e where T_e will be given as an output from the UDC-Control loop. Further the DTC will be able to assure a high power factor by controlling the reactive power.

As there are many types of drive control, the applied principle in the AR is Direct-Torque-Control (DTC) without position sensors. It stands in contrast to the widely applied Vector Control which had been first presented in 1968 by K. Hasse, Darmstadt, Germany [27]. DTC was invented in 1985 by Manfred Depenbrock who at that time

worked at *Brown, Boveri & Cie (BBC)*, Mannheim, Germany. Almost at the same time, Isao Takahashi presented similar ideas in a Japanese journal [27].
From a historic point of view, DTC has been commercially implemented very late. In 1995 the first industrial drive with DTC for induction motors was available.

Features of DTC are:

- Stator flux and electromagnetic Torque are controlled directly
- Reduced torque oscillations (claimed)
- Excellent torque dynamics (claimed)
- No fixed switching frequency
- Reduced number of switching actions
- No coordinate transformations needed

The reason for choosing this specific type of AR was the ability to control the generator with a high pole-number in speed-sensorless operation as this requires highly developed estimation methods in drive control.

Both, vector control and DTC rely on a space-phasor model of an electric machine. In space phasor theory the three stator phases are being transformed into a model with two phases. Applying the right equations the controlled parameters Ψ_R and T_e can be estimated by measuring generator phase voltages and phase currents. Most common for DTC schemes is a tolerance-band control that will point the error value to a look up table. From that on the references and real values are compared. As for example the flux can be a function of the voltage, the right voltage vector is chosen out of the table. According to various control schemes there can be a variety of look-up tables in such DTC drives.

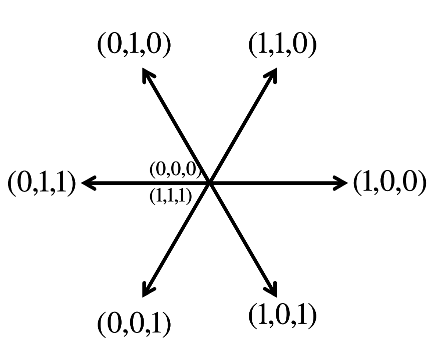

4.7-8 Voltage vectors of a 6-pulse inverter

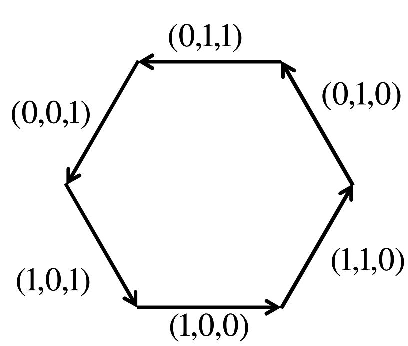

4.7-9 Possible switching sequenc

By applying this principle, the flux created in the stationary reference frame (αβ-system) could look as following:

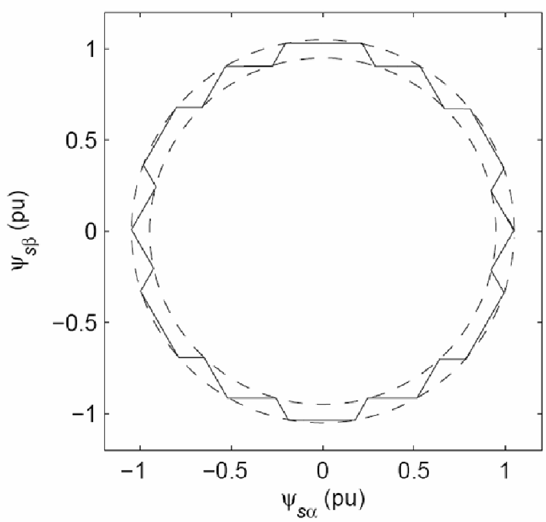

4.7-10 Possible flux circle created by a DTC algorithm

If one now would like to control the power factor for example, the DTC algorithm could employ a look-up table that according to the present values of power and speed could increase or lower the inverter voltage by which the current could be aligned to the actual voltage value produced of the PMSG.

4.7.4 DC-Link Control for Battery Charging

As chargers for that battery size are rather expensive it could be worth to see if charging via the DC-link could be an option. Basically, to meet the charging demands of a lead-acid type battery we need to control the battery current and the battery voltage over a certain time [1]. While the basic logic for the charging algorithm could be put into the system control the electrical control could be performed by the AR. If the charging mode was activated, the UDC-voltage would simply be regulated to the lower battery charging voltage.

The electric circuit for charging a battery by the DC-link will look as following:

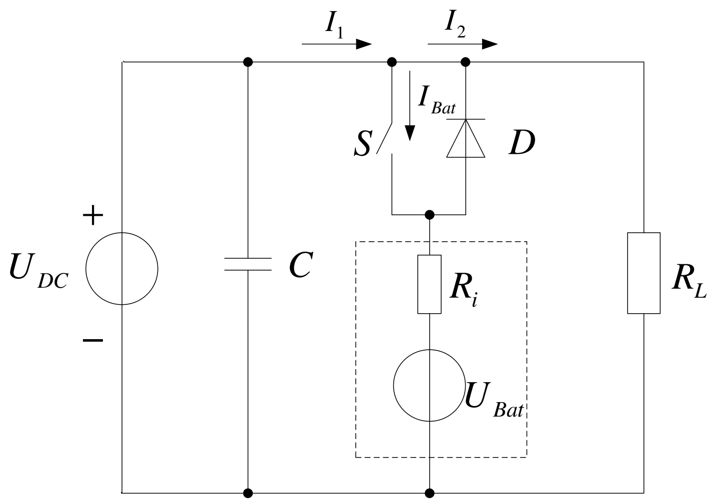

Figure 4.7-11 Schematic for battery charging via the DC-link

The charging procedure will be activated by closing switch S if the system is in stable operation. It can be seen that the charge current I_{Bat} can be derived by subtracting I_2 from I_1 which both are being measured by the AR and the INV. Further I_{Bat} will be dependent on the voltage over the battery clamps. Much attention has to be paid on the charging voltage to meet the maximum ripple specification hence to allow for charging lead-acid batteries. The voltage ripple measured over the batteries terminal will give information about how much ripple current will be dissipated in the internal structure (generally internal resistance) of the battery. If the energy caused by the ripple currents is too high, battery life will be dramatically reduced as internal structures will be deconstructed much faster. Therefore as an indicator the measured voltage ripple should not exceed 1.0 % (rms) of the float voltage level while charging and 0.5 % (rms) at trickle-charging [1].

To find out if these specifications for the RMS-voltage ripple can be met, measurements on the HPS need to be carried out. A HPS with 30 kW nominal power will basically be used at average loads of 10 kW. To have some margin, the test will apply 12 kW of load to the system where 10 kW will be shared by the battery. The results for the voltage ripple measurement are taken from chapter 5.

	Value	Unit
Battery Float Voltage	436	VDC
Peak-to Peak Voltage	5.8	V
Mean Voltage	-192	mV
RMS Voltage	924	mV
Burst Width (typ.)	8.2	ms
Referenced RMS Ripple	**0.22**	%

4.7-1 Results from measurements performed on the DC-Link with 10 kW battery share

Finally, the table above shows low value of only 0.22 % for the RMS-Voltage Ripple referenced to the battery floating voltage of 436 Volt. As a result of these measurements tests on real batteries should be performed to compare the true behaviour of the batteries to the expectations.

Not considered have been overshoots that can occur if loads are connected that behave like a step-type load. These non-steady-state errors can be rather big but probably would not occur that often. As this problem strongly relates to the connected load no real predictions are possible here.

4.8 System Control

The expression *System Control* represents all high level control for operating the HPS and its components. Sometimes also “Overriding System” is used to express this functionality. Usually, system control is implemented in a PLC (Programmable Logic Control) or an IPC (Industrial Personal Computer).

4.8.1 Specification of a New System Control

The following tasks appear for the new System Control:

- AR **and** INV Control over Ethernet (new)
- External Charger Control
- Diesel Genset Control
- Auxiliary Power Source Control[1] (new)
- Remote Control (new)
- Data Logging (new)

As the old PLC has become obsolete and the communication to the AR and INV has changed to ModBus over Ethernet a new solution has to be found.
Thus, the decision has to be made either the PLC or the IPC solution suit to the application.

[1] Future auxiliary power sources can be Photovoltaic, Fuel-Cells, etc.

4.8.2 Comparison PLC and IPC

Basic criteria for the comparison are cost and flexibility of each solution. Of course all tasks defined in the specification should be met.To get a good overview, a table is provided below:

	PLC	IPC
Meet all specifications?	yes	yes
Flexibility in Hardware?	yes	yes
Flexibility in Software?	yes	yes
Cost Software?	already acquired	high
Cost Hardware?	very low	high
Effort and Complexity?	low	high

Table 4.8-1 Comparison of PLC-/IPC solution for system control

The comparison shows clearly that the PLC solution has advantages over the IPC solution. In case the software development will be carried out by the company itself the PLC solutions should be preferred. Even though, an external software company could prefer to work with IPC technology, the drawback could be that quick modifications to the HPS software could cause extra cost and the programming knowledge will be given away. Having that in mind, the PLC solution at least seems to be a very good choice.
Finally the components for a PLC setup have been ordered and used further on.

4.8.3 System Communication

The new System Control with a PLC will apply Ethernet communication. Usually these networks have a star-topology applied. The centre of this star-point is an Ethernet-switch, by that the following communication layout will be achieved:

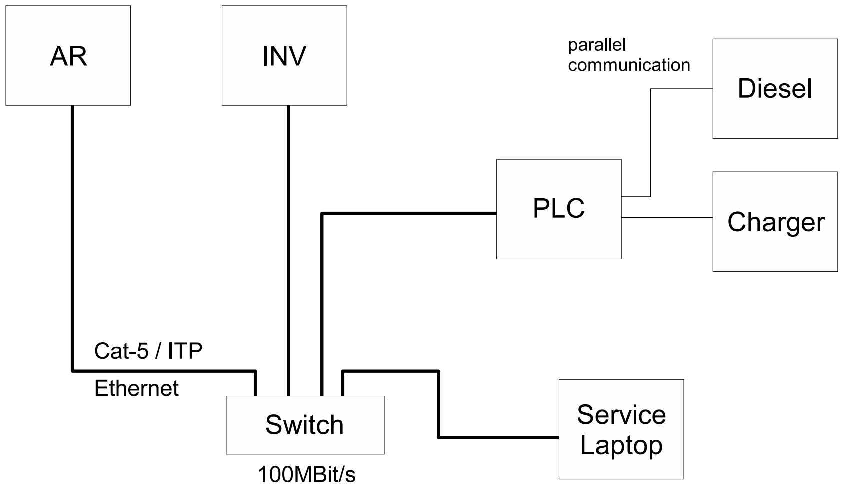

Table 4.8-2 Communication Layout for the HPS

The first task to set up a communication is to know and configure the network-layers in the specific application also known as protocols. As Modbus/TCP will be applied, the communication between two devices will look as following:

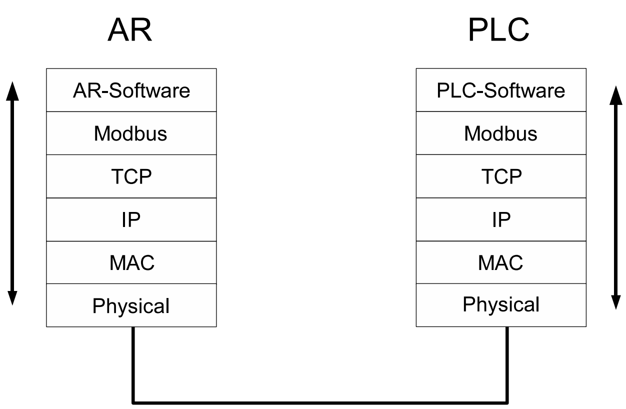

Figure 4.8-1 Communication example for two HPS-components

Regarding the complete protocol stack, not all layers need full configuration. By defining the network speed to 100MBit/s the first configuration needs to be done in IP-protocol.

In IP-protocol so called IP-addresses are given to all network devices. An IP-address consists of two parts:

Network-Address | *Host-Address*

According to IPv4 standart this combined address will consist of 32 bits while the share for Network- and Host-addresses remains flexible.
By defining the network as local (non-public) network a Class-C addressing should be used. To specify Class-C network addresses the subnetmask has to look as following:

Subnetmask (Class-C): 255.255.255.0

The subnetmask represents a binary mask to separate network address from device address. By processing a binary AND command both address-blocks from an IP-Address can be obtained.

Binary Subnetmask: 11111111 11111111 11111111 | *00000000*
Network-Address-Block *Host-Address-Block*

The non-masking last byte is available to address devices where eight bits will result in a maximum of 256 addressable devices (0-255).
Now, IP-addresses for all network devices need to be found. The standard RFC 3330 gives a recommended range of IP-addresses for private (local) networks:

Recommended IP-block for private networks: 10.0.0.1/8

	IP-address
AR	10.0.0.10
PLC	10.0.0.11
Service-Laptop	10.0.0.12
Gateway	10.0.0.1

Table 4.8-3 IP-Addressing for a HPS (example)

It has to be noted, that the use of DHCP (Dynamic Host Configuration Protocol) functionality for automatic addressing and network configuration should be turned off. This assures defined IP-addresses for the same devices under any circumstances.
The Gateway address will be used in case a modem, calling for a Gateway address is being added to the network.

As soon as all cabling and configuration work is done, the network is ready to operate, at least until the TCP layer. Still, the Modbus-communication of each device has to be investigated. Therefore the specific manuals should be studied to get to know, which specific modes are supported.
Basically, Modbus/TCP is a relative of Modbus/RTU (Remote Terminal Unit). A basic Modbus message looks as following:

Slave Address	Function Code	Data	CRC
1 byte	1 byte	0..252 byte(s)	2 bytes

Figure 4.8-2 Frame description for a Modbus message

For a properly working modbus communication the network hast to be split up in masters and clients. The modbus-master will serve the communication while coordinating write/read-commands from/to the slaves. In this case, the modbus-master is the AR. The PLC will act as a modbus-client.
To exchange the correct data, the PLC internal "ethernet-coupler" and the communication function ETH_MOD_MAST (contained in a modbus library) needs to be configured carefully. Important parameters to check for each device are:

- Number of Modbus Clients
- Supported Modbus Read/Write Functions
- Modbus-Address of the Data
- Datalength (number of transmitted words)
- Datatype
- Address

Information on that can be found reading the manuals from all suppliers carefully.

4.8.4 System Control Software

The system control software is written and compiled in standart PLC software recommended from the PLC supplier. Not all parts of the program have been written by the author. For optimal operation of the software there needs to be a good software architecture, otherwise runtime errors will occur. Basically a program scheduler is needed to call the right sub-routines. Some tasks need quick execution others need to be checked less frequently.
The structure for the System Control Software will look as following:

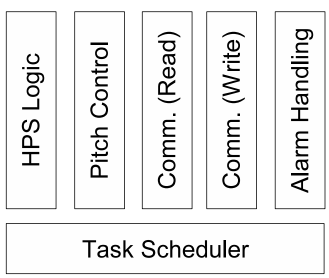

Figure 4.8-3 Structure of the System Control Software

To get external access to internal variables/parameters of the System Control Software it has been decided to put them in memory regions that can be addressed by using Modbus-addressing. By that, it is possible to use more simple software, connect a laptop via Ethernet and check/edit parameters in the system control software out in the field.

4.8.5 System Control Test

To test the software and the components a test setup has been set up. The Modbus communication between PLC and the AR / INV was tested by checking with two computers connected to the devices. Other functionality of the HPS e.g. pitching was tested with the connected periphery which simulated the real hardware.

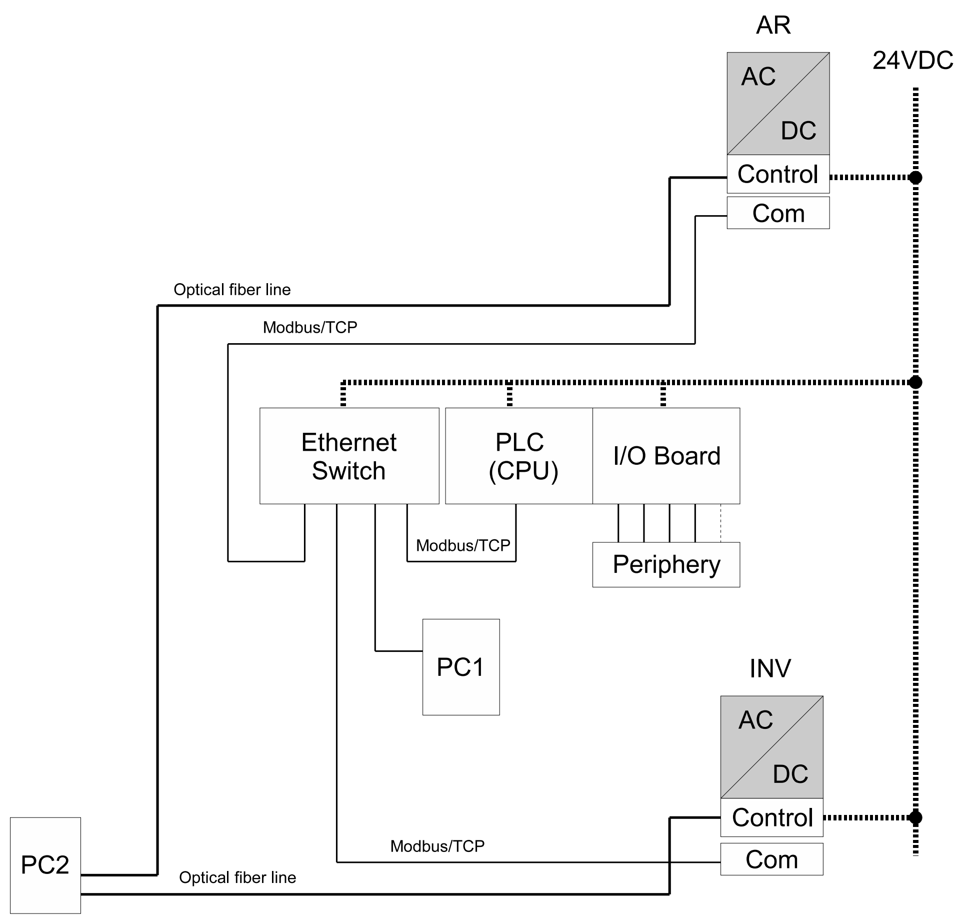

4.8-4 Test setup for the system control with a PLC

5 Measurements

5.1 Measurement Setup

The system for taking measurements has been set up as illustrated below:

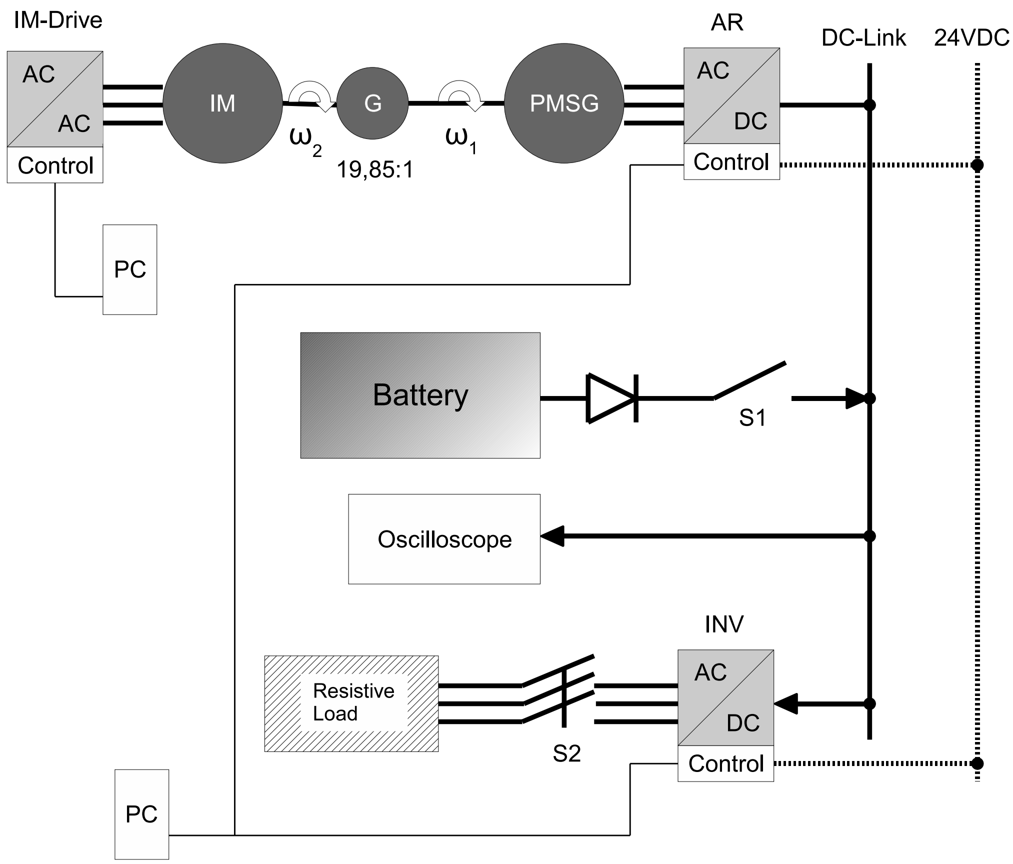

5.1-1 Measurement setup for the HPS at Chalmers machine laboratory

The following measurement equipment has been used:

- Tektronix THS720P, fully isolated digital Scope
- In-build measurement devices of the AR
- Two PCs for control and data acquisition

5.2 UDC-Control

5.2.1 Adjusting the PI-Controller

Many tests have been done to prove safe operation of the PI-controller. Some example tests can be seen below. For the tests both AR and INV are activated, the stepload will be applied by directly switching a resistive load on the three phase output of the INV and observing the DC-Link voltage. The controllers' integration part equals always 8000 and only the proportional value will be altered.

The most values shown are scaled and allow no value reading, the y-axis instead will always show UDC/2.

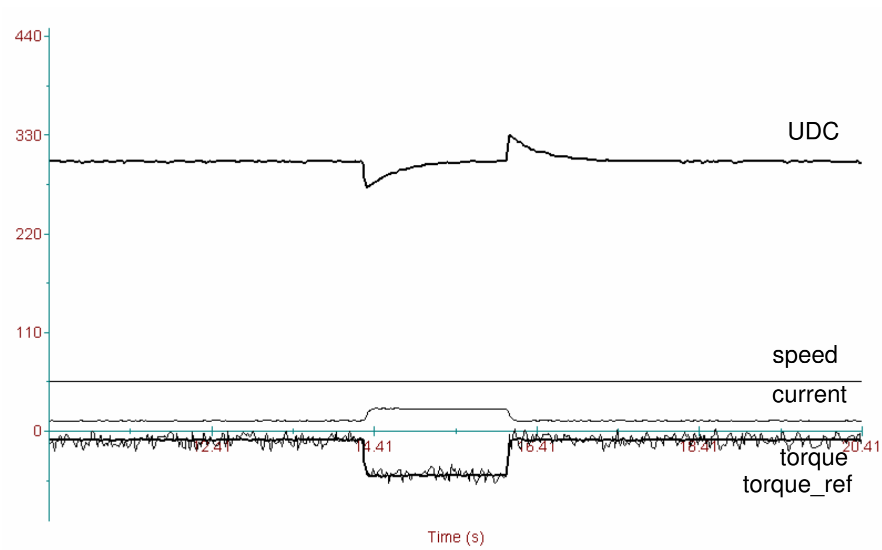

5.2-1 Stepload 1 kW, UDC= 600 V, i= 8000 p= 3000

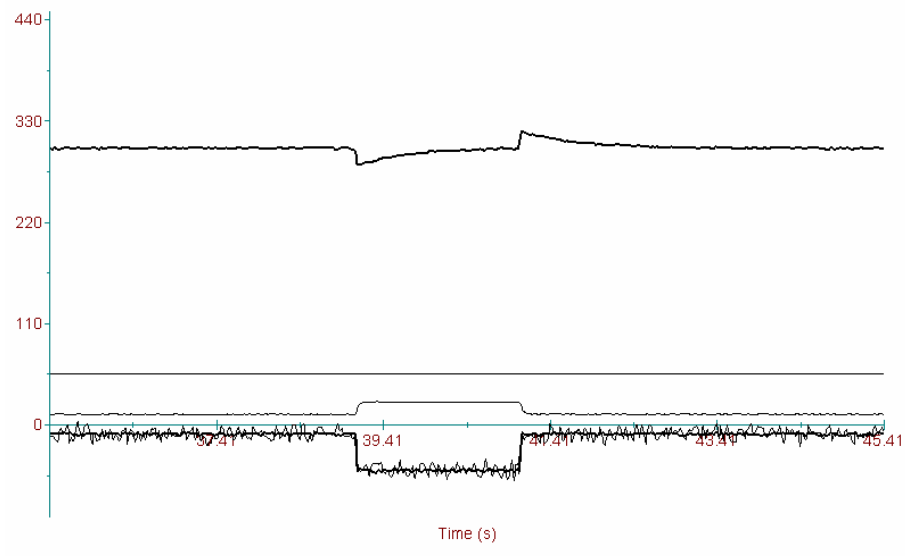

5.2-2 Stepload 1kW, UDC= 600 V, i= 8000, p= 5000

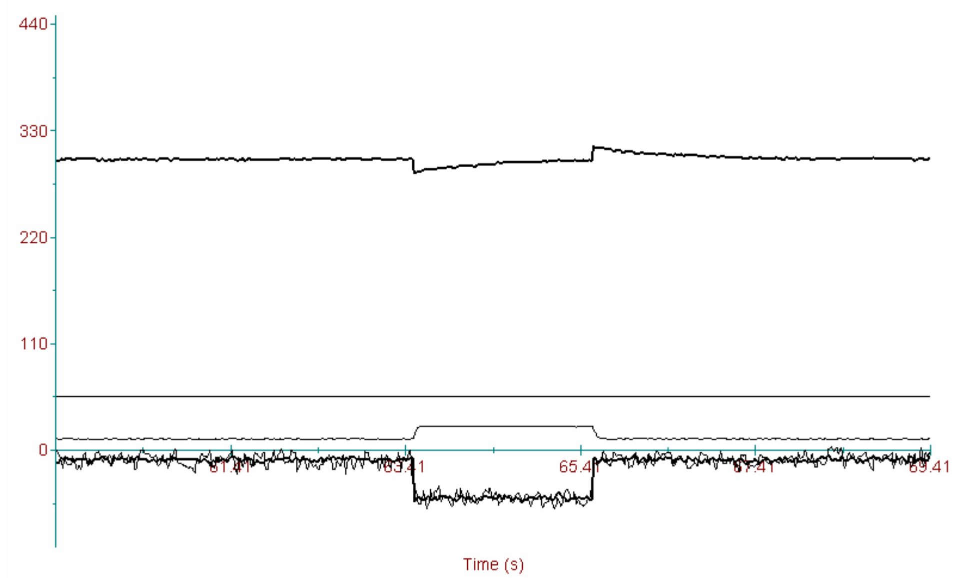

5.2-3 Stepload 1kW, UDC= 600 V, i= 8000, p= 7000

Further increases are not recommended as they will influence the start-up behaviour. Usually start-up happens very smooth, though, there has been detected a special behaviour around 70 rpm.

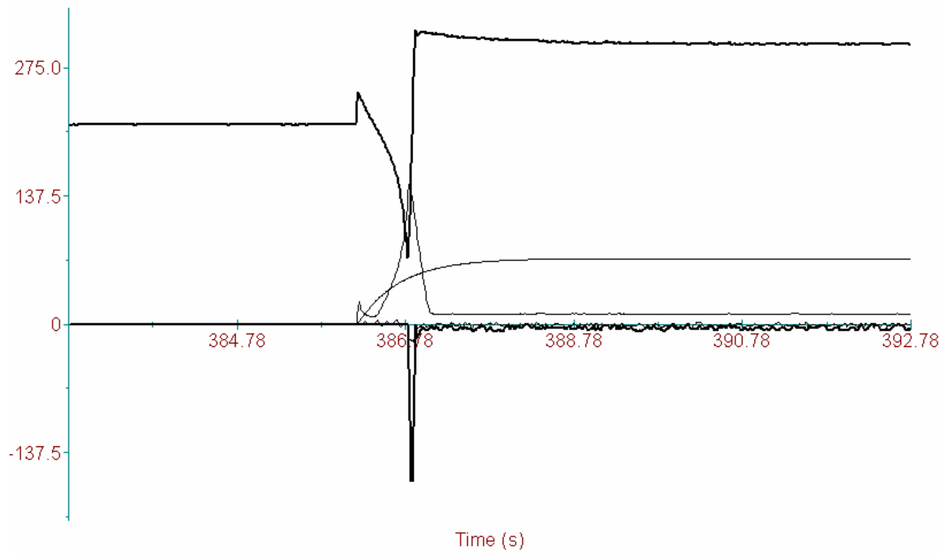

5.2-4 Start-up at 70rpm, i= 8000, p= 7000

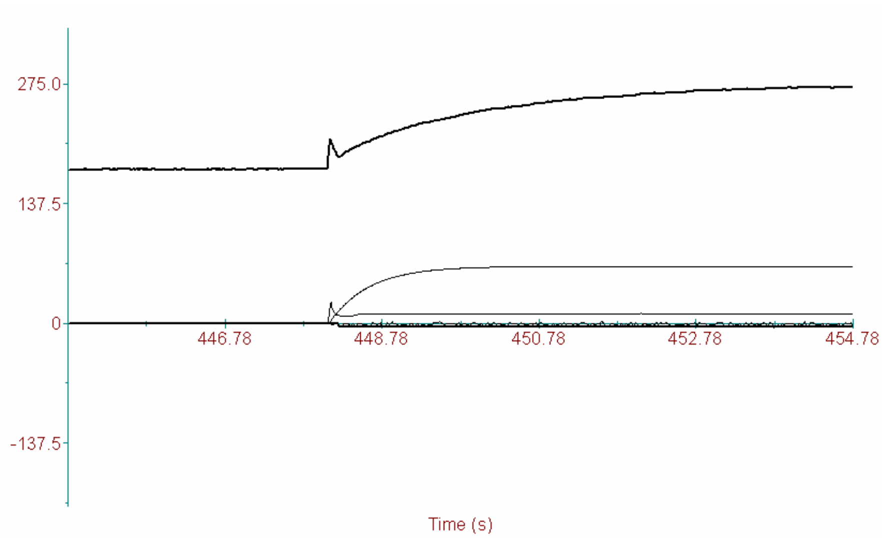

5.2-5 Start-up at 65rpm (similar to all lower speeds down to 45rpm), i= 8000, p= 7000

5.2.2 Complete AR-Startup (without battery)

A full AR-startup consists of two stages. In Stage one the drive will start to track the generator and tries to take over full control. For this stage a programmed torque will be taken to provide power for the AR’s power electronics. The reason is a possible system operation without batteries. This could happen if the batteries need to be replaced. Stage two will be the start-up of the UDC-control and is only performed after successfully passing stage one.

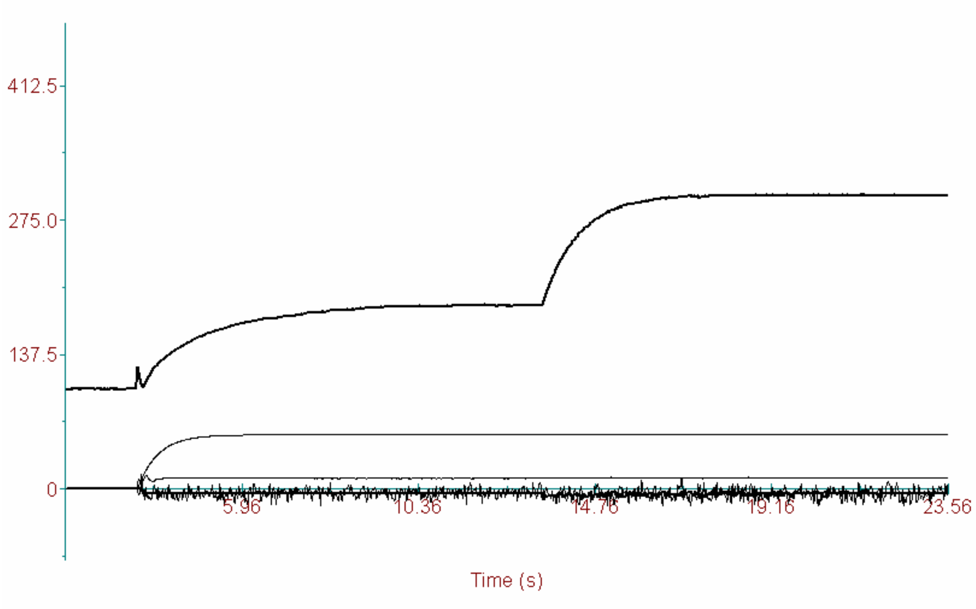

5.2-6 Complete AR-Startup, without batteries (stage two elevates UDC to 600 VDC)

It was found, that the internal measured UDC values provided by the AR are strongly filtered. Therefore it is necessary to look also with an oscilloscope. First measurements with a standard oscilloscope and a differential probe did not give any usable values. It seems that the differential circuit is not good enough to cope with the highly floating DC-Link. For that reason a fully isolated and battery-powered scope was taken.

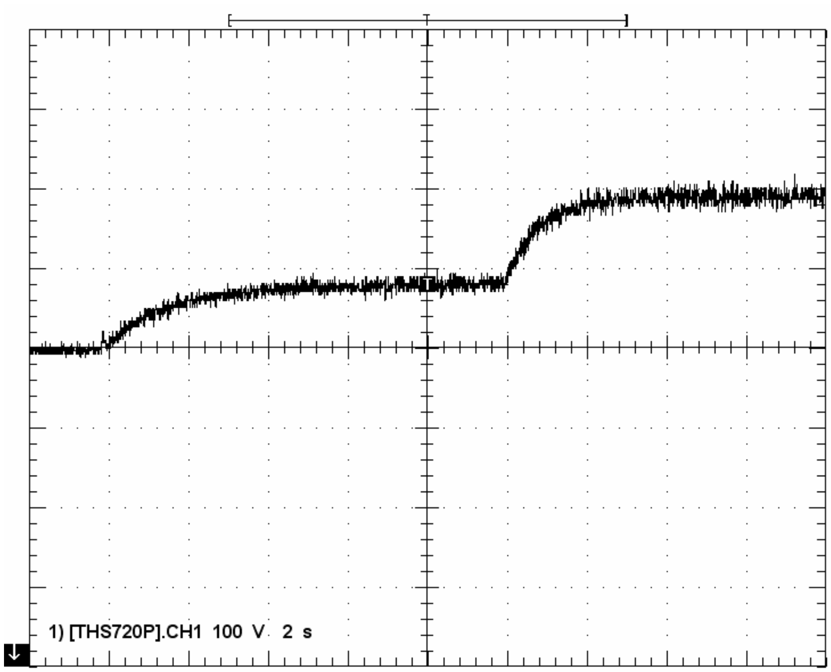

5.2-7 Complete AR start-up showing the two stages (isolated scope)

5.2.3 Step-Load Tests (without battery)

The following graph will show a step from 0 kW to 10 kW of load.

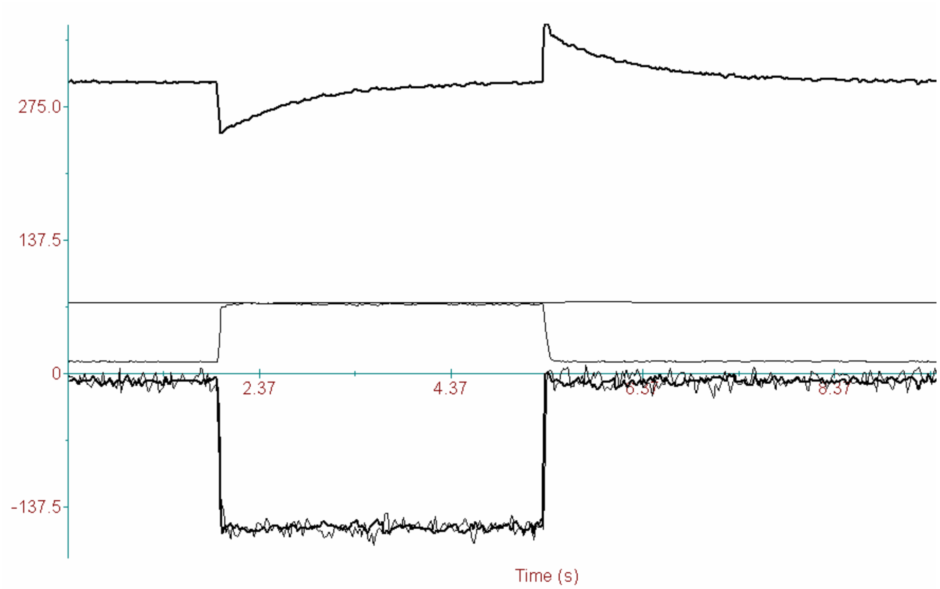

5.2-8 Step-load 0 kW to 10 kW

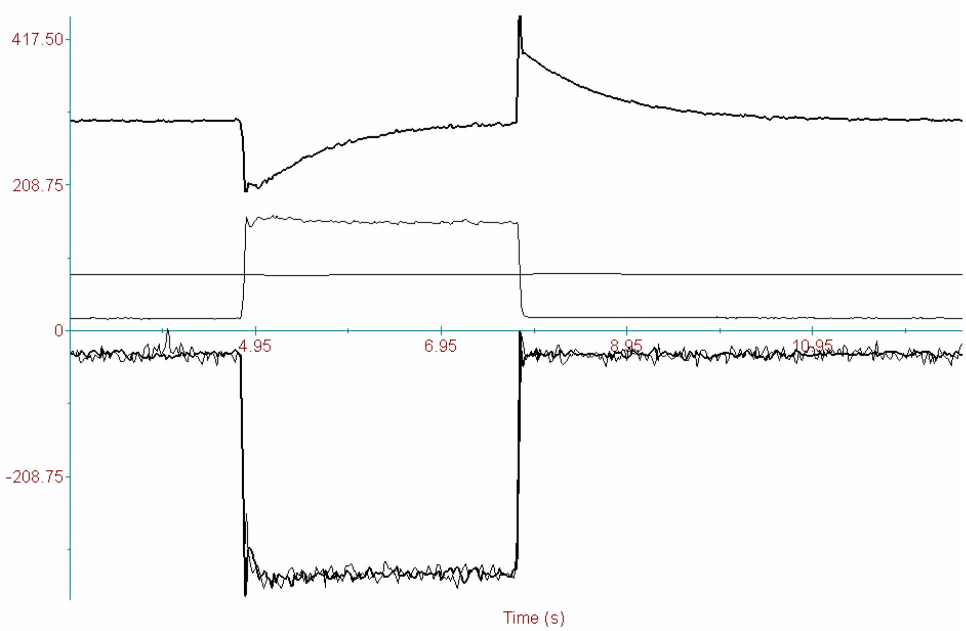

5.2-9 Step load 2 kW to 20 kW

From the leading edge of the motor torque curve it can be seen, that the integration part of the PI-controller hast just the right value. A further increase would cause the system to torque oscillations.

5.2.4 Load Tests with battery

The load tests with a battery connected will show the behaviour of a real hybrid power system where the diesel generator is not started.

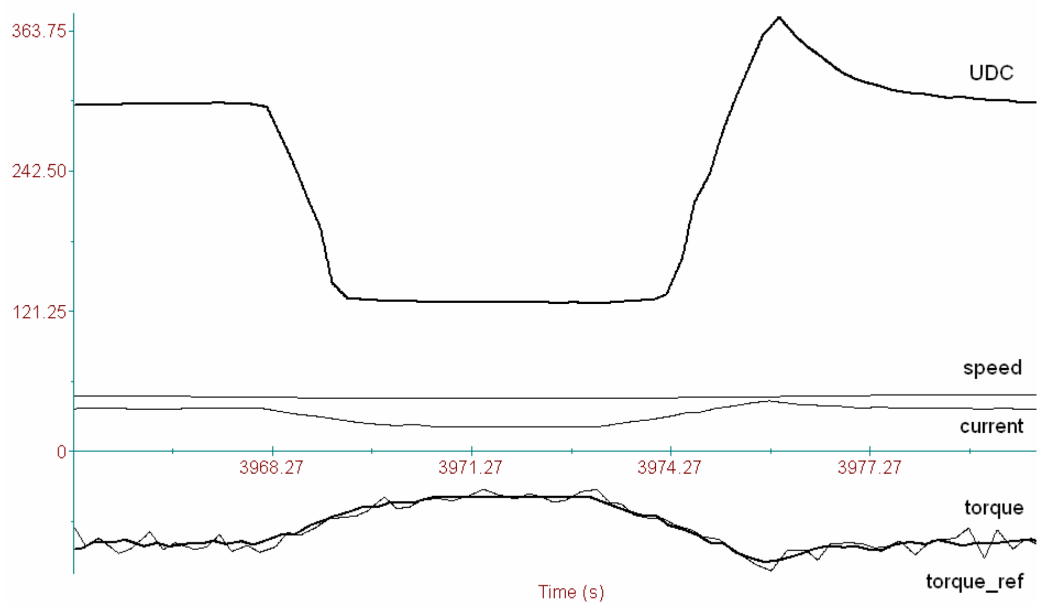

5.2-10 Transition from wind power to battery power and back to wind power, unloaded

To create the picture above the generator speed has to be lowered until the power from the turbine is not enough to establish the 600 Volt DC-Link any longer. Suddenly the DC-Link voltage drops to the battery level. By increasing the speed, the UDC-Control will start to set up the programmed DC-voltage again. In this test, the system was unloaded to see how the PI-Controller regulates the DC-voltage, obviously while coming back from battery to wind-power there is an overshoot.

The same test has been performed with a load step from 2 kW to 12 kW without changing the turbine speed which was adjusted to supply 2 kW. The result looks as following:

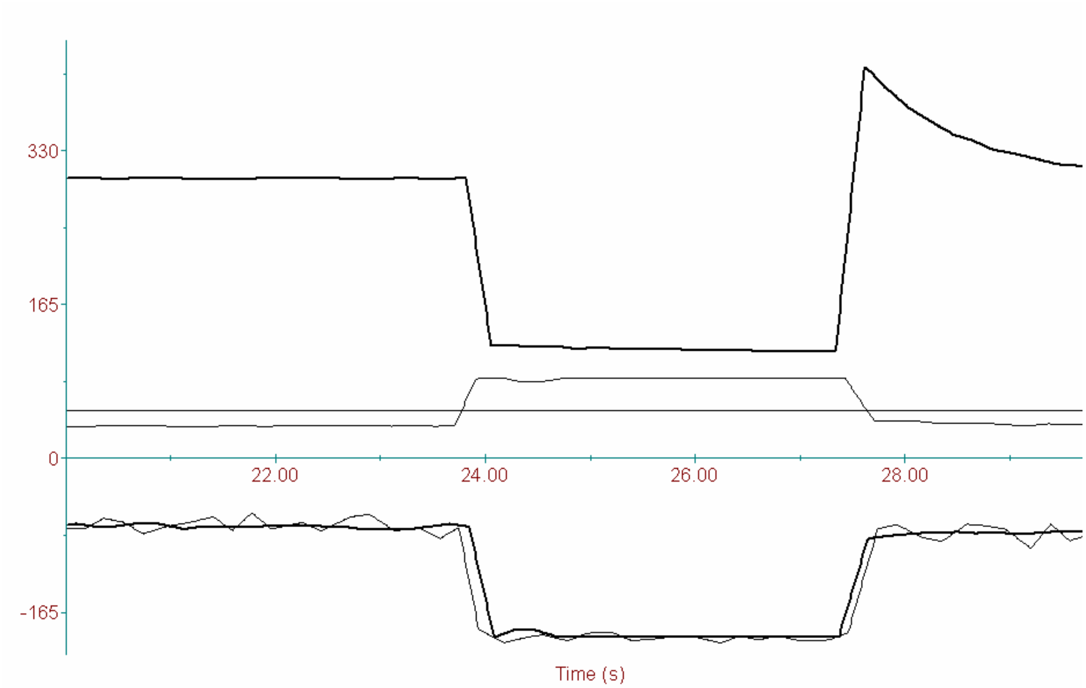

5.2-11 Transition from wind power to battery power and back to wind power, fixed speed with step load 2 kW to 12 kW

The graph shows, that there is still an overshoot when coming back to operation on wind power. In case there would take place a charging of the batteries via the DC-Link the UDC voltage would be controlled close to the float voltage of the batteries. There, no such overshoots are being produced.

5.3 PPT-Control

The following graph is showing the turbine start and a turbine stop. By that, the principle of the PPT-control can be seen. To create that graph, the System needs to be fully loaded otherwise the UDC-Control will not take out the full power that is programmed. Because of the generative mode, the torque curve is showing negative values. All values except the turbine speed are scaled. The y-axis shows true rpm values. The reached speed in this test is 75 rpm.

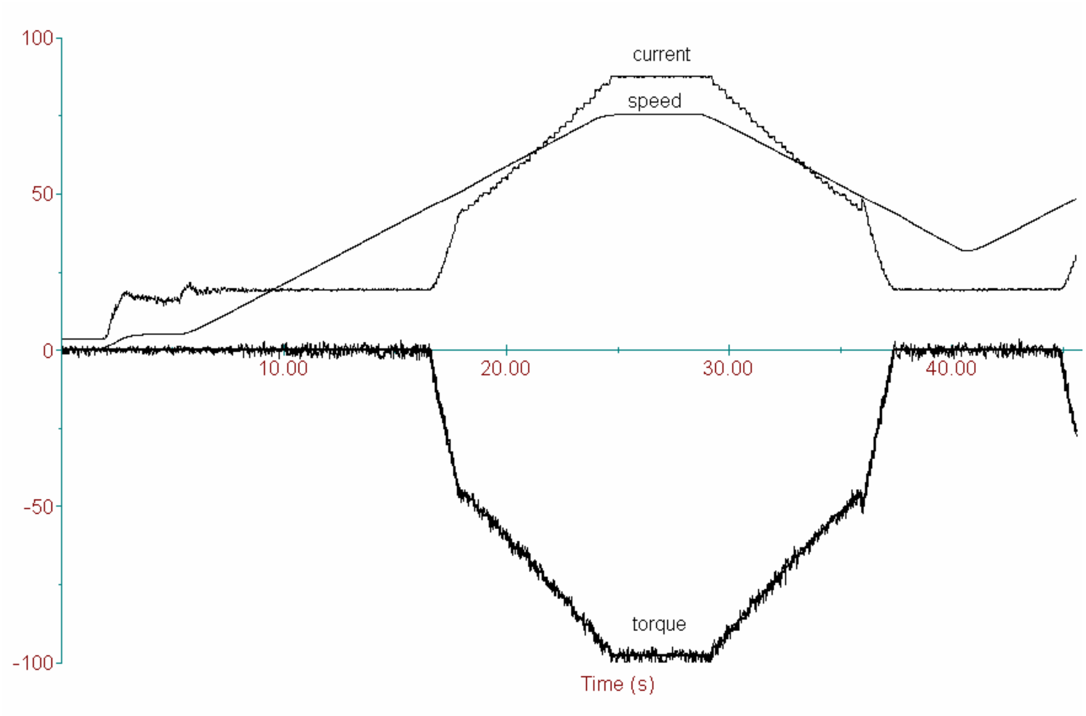

5.3-1 Turbine Start and Turbine Stop showing the torque commanded by the PPT-Loop

5.4 DC-Link Quality

DC-Link ripple measurements were taken to see:

- How good the UDC-Control is working
- How the INV switching influences the DC-Link
- How much voltage ripple the batteries will experience
- If charging of the batteries could be an option

Note that one square represents 1 Volt difference in the graphs below.
Time base will usually be 50ms for each square. All graphs are AC referenced and therefore show no UDC-level.

5.4.1 DC-Link unloaded

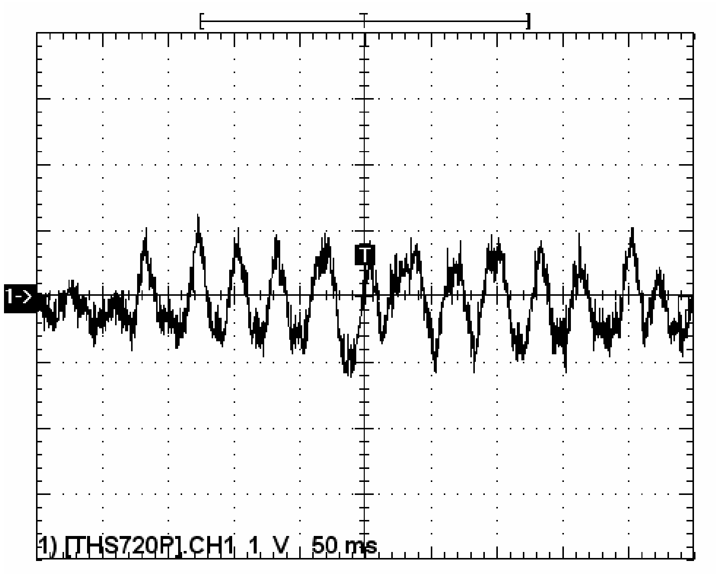

5.4-1 DC-Link ripple voltage – AR operating only

If only the AR is operating the average voltage ripple observed was about 2 Volt.

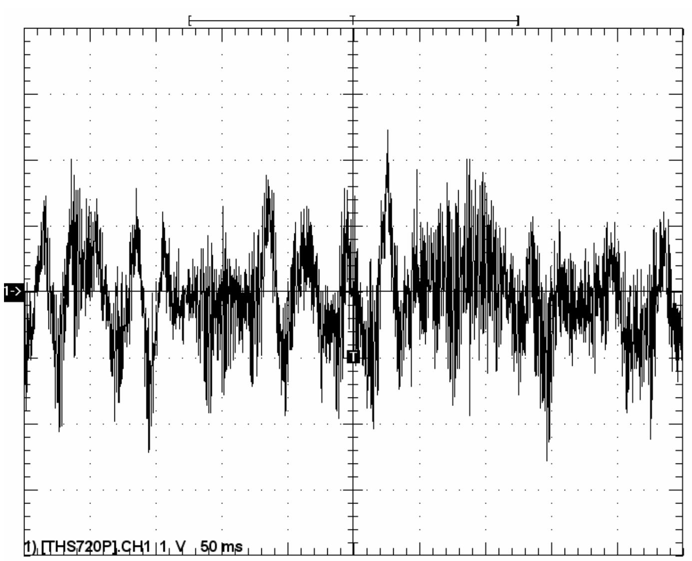

5.4-2 DC-Link ripple voltage – AR and INV operating

Suddenly there are much more high frequency components by switching on the INV. Also the average ripple voltage reaches about 3 Volt now.

5.4.2 DC-Link loaded without battery

The DC-Link will be loaded from the inverter-side now.

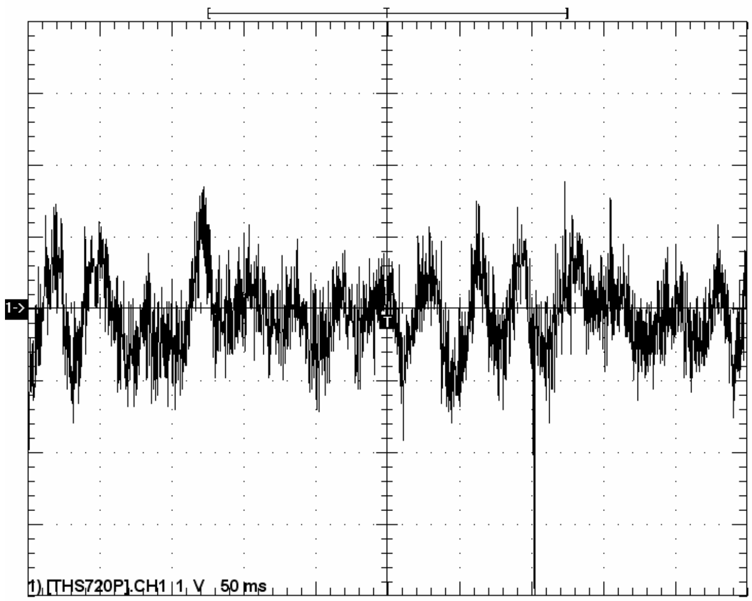

5.4-3 DC-Link ripple voltage – 2 kW load

Compared to the no-load test - the 2 kW load does not have a major impact on the DC-Link. The load will be further increased to 10 kW for the next graph.

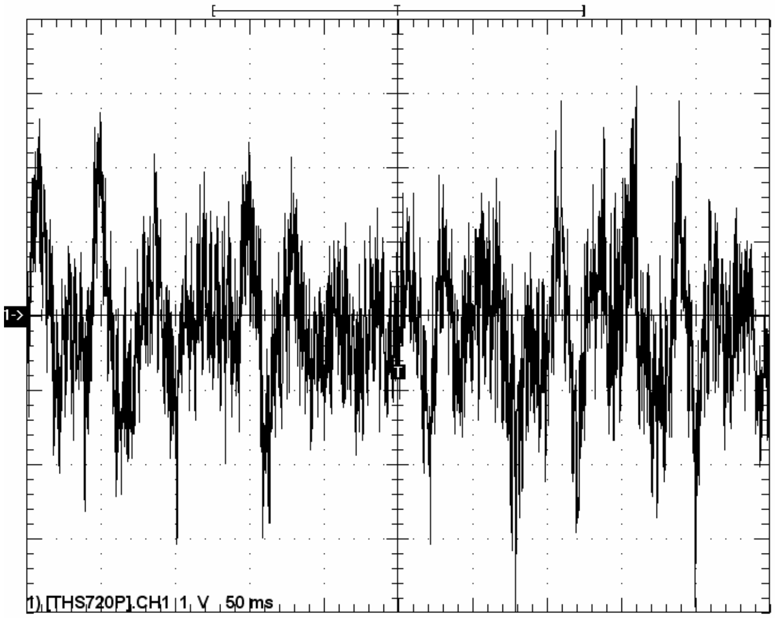

5.4-4 DC-Link ripple voltage – 10kW load

Suddenly, there is a difference, the voltage ripple reaches about 5 Volts in average.

5.4.3 DC-Link loaded with / without Battery

An interesting comparison is to see the immediate difference between a loaded DC-Link having a battery connected and having it disconnected.
To see this difference there have been made two tests with the same load of 2 kW but different turbine speeds to toggle between turbine power and battery power.

The first graph will show the DC-Link without interacting of the battery:

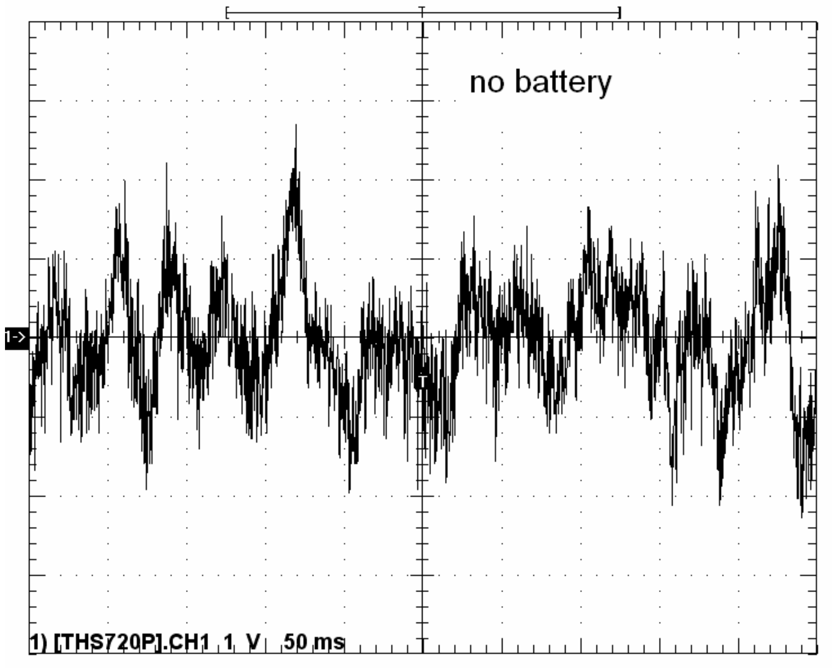

5.4-5 DC-Link ripple voltage, 2 kW load, no battery

The same conditions now by running on battery:

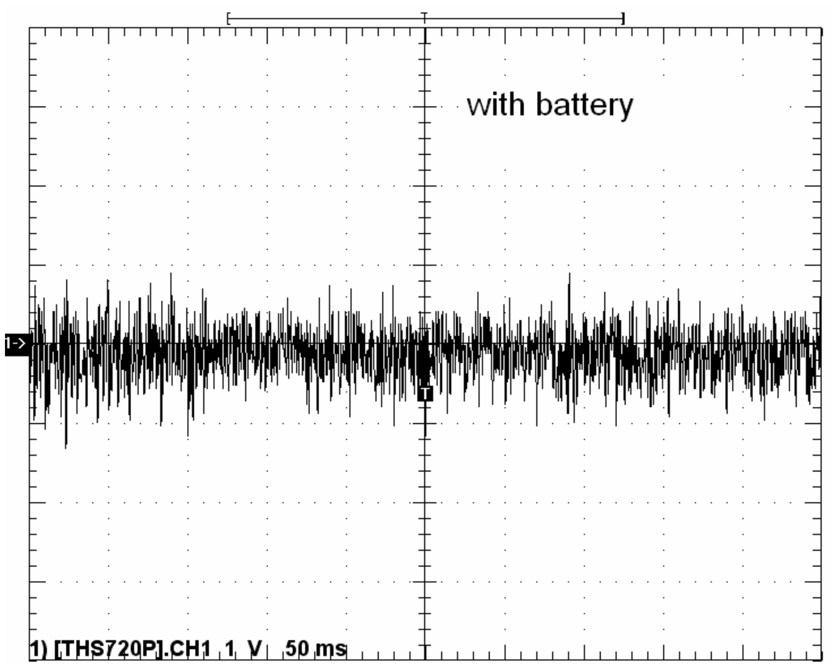

5.4-6 DC-Link ripple voltage, 2 kW load, battery connected

Comparing the two figures above shows the clear difference, although tests with higher loads indicate that the smoothing effect of the battery will be somewhat reduced.

An important measurement will be the DC-Link quality while most typically loaded to define if charging via the DC-Link can be possible. A HPS with 30 kW nominal power will basically be used at average loads of 10 kW. Therefore the following test will apply 12 kW of load to the system where 10 kW will be shared by the battery. For this measurement a calculation of the RMS-voltage present on the AC referenced DC-Link will be made.

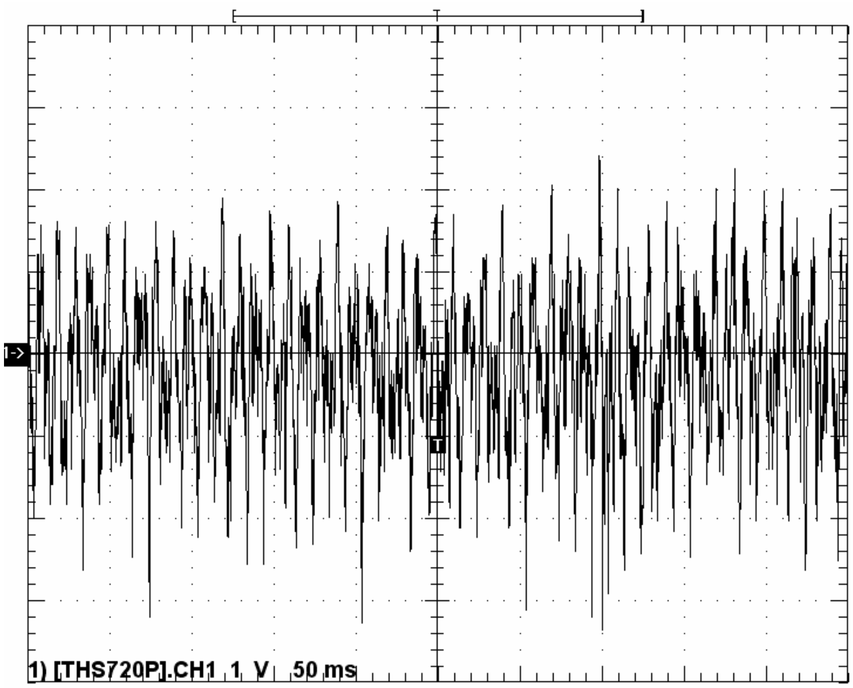

5.4-7 DC-Link quality for 12 kW overall load, where battery load share is 10 kW

The following values have been calculated with WaveStar® 2.8.1 software:

	Value	Unit
Peak-to Peak Voltage	5.8	V
Mean Voltage	-192	mV
RMS Voltage	924	mV
Burst Width (typ.)	8.2	ms

5.4-1 Measured Values for DC-Link loaded with 12 kW and 10 kW battery load share

The interpretation of these values can be found in chapter 4.7.4.

6 Conclusions / Future work

Regarding other types of renewable power sources for a HPS there is a limited choice of components for systems in 30kW power range. Reasonable configurations should contain reliable wind- or solar power devices depending on the local conditions. Special technologies will seldom fit to the demands of robust autonomous power systems in lower power ranges.

As an alternative for the actual Pitchwind 30kW turbine the Eoltec Windrunner 25kW turbine was found to be a good choice. Comparisons showed advantages in: robustness, fewer maintenance, weight, system efficiency and cost. Nonetheless, careful tests would be needed to prove the claimed abilities of this turbine on the field.

The comparison of active- and series compensation clearly shows no advantage for series compensation on all regarded aspects. The actual active rectifier remains a very good choice for the system application. Future work could also investigate on how the efficiency of the PMSG could be increased by allowing a certain amount of reactive power in the machine.

The implementation of a new turbine control has been successfully completed. The new control shows superior behaviour compared to the old control. As an advantage over the old system a big and expensive external capacitor bank could be avoided.

The comparison of a PLC and IPC solution for the system control showed that using a PLC solution would have more advantages over an IPC solution and therefore is clearly recommended.

Also, the system control has been successfully implemented. Tests show the working Modbus communication from the PLC to the AR, though, some minor fixes have to be done as one part of the code does not show expected behaviour.

The exciting feature of charging lead-acid batteries via the DC-Link could be a promising task to be implemented and would safe an additional expensive charger unit. Tests on charging batteries are recommended.

Unfortunately, multi-turbine operation could not be tested in the given time frame. Still, the implemented UDC-control allows to set up each AR for multi-turbine operation. So far, the lab has been prepared to carry out these tests.

In general it should be noted, that all tests have been performed in a lab environment – therefore, full testing on site locations should go on.

Appendix A

Technology	Footprint	Area	Total Annual Energy
WEC	250 x 250 m^2	62500 m^2	14 230 MWh/y
PV	10 x 1 m^2	10 m^2	2 000 kWh/y
HCPV	72.2 x 72.2 m^2	5227 m^2	1555 MWh/y
OWEC	158 x 158 m^2	25000 m^2	2628 MWh/y
SWEC_1	30 x 30 m^2	900 m^2	100 MWh/y
SWEC_2	26.6 x 26.6 m^2	709 m^2	78.7 MWh/y

Table 5.4-1 Area and annual energy specifications for different technologies at preferred locations, data acquired from manufacturers and [15], [19]

Installation Type	Energy consumpt.	Energy product.	Energy amortisation
V90-3.0 MW onshore	4,311 MW	157,800 MWh	6.6 months
V90-3.0 MW offshore	8,098 MW	284,600 MWh	6.8 months

Table 5.4-2 Vestas energetic facts of V90 Turbine, Vestas 2004 [12]

System	Net-Power	Total System Costs	Cost per 1kWp installed
Vestas V90-3.0 MW, offshore	3 MW	5 Million €	1667 €
Solarworld SunModule	1 kW	3900 €	3900 €
Solar Systems CS500	720 kW	1.49 Million €	2065 €
OceanPowerDelivery Pelamis	750 kW	1.25 Million €	1866 €
Pitchwind System 30kW	30 kW	90 000 €	3000 €
Eoltec E11-25	25 kW	78 000 €	2720 €

Table 5.4-3 Data acquired from manufacturers, sales companies or published contract data (prices excl. VAT)

Technology	Annual Energy per m^2	Installation Cost per 1 kWh
WEC	228 kWh	0.0175 €
PV	200 kWh	0.0975 €
HCPV	298 kWh	0.048 €
OWEC	105 kWh	0.0238 €
SWEC_1	111 kWh	0.045 €
SWEC_2	111 kWh	0.0495 €

Table 5.4-4 Annual energy production per m^2 and cost per 1kWh (assuming 20 years life-time)

Appendix B

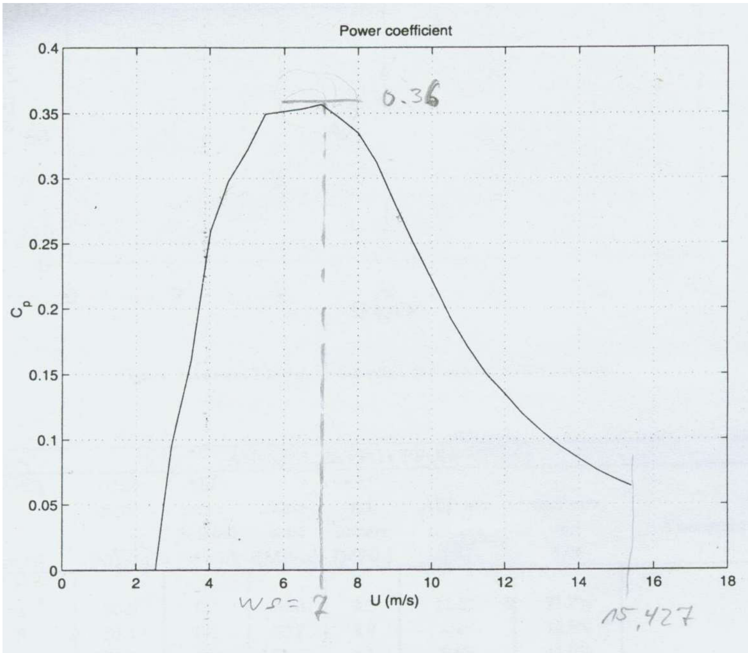

Figure 5. Power coefficient as function of the wind speed

Figure 5.4-1 Figure 5 of FFA report showing electrical power coefficient for PW14-20

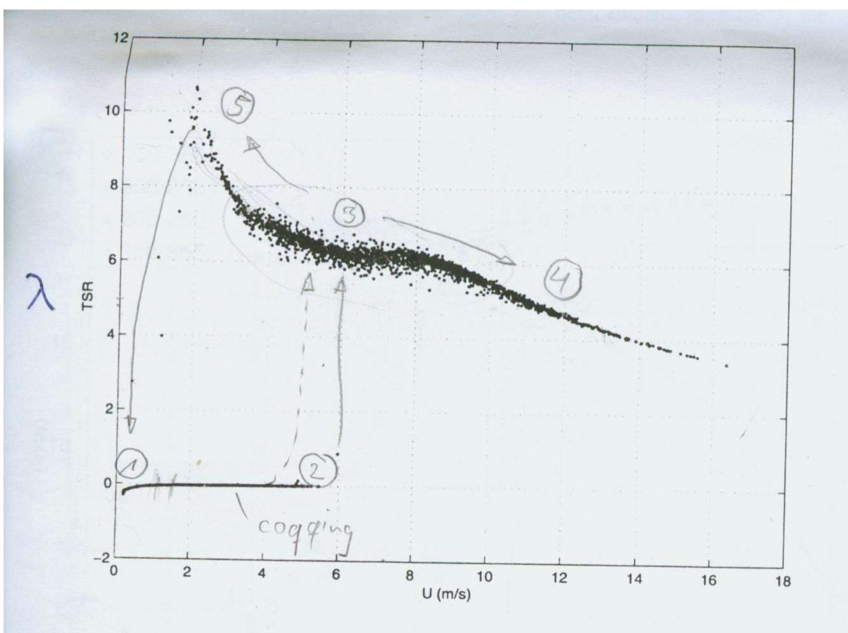

Figure 6. Tip speed ratio for different wind speeds

Figure 5.4-2Figure 6 of FFA report showing lambda over different wind-speeds for PW14-20

system losses:	
eta_gen	0,86
eta_rect	0,97
eta_inv	0,97
eta_filt	0,98
eta_system	0,792991

Table 5.4-5 Assumed efficiencies of components installed during FFA power measurements and further back-calculation

n_gen	P_turb	S_turb	PowerFactor
	(KW)	(kVA)	
27	0,55	1,00	0,56
37	1,52	1,77	0,86
47	3	3,1	0,97
57	5,2	5,2	0,99
67	8,3	8,4	0,99
75,7	13,3	13,5	0,99
75,7	15,5	15,8	0,98

Table 5.4-6 Power Factor measurement for Active-Rectifier-Setup

Used equipment:

- NORMA Wide Band Power Analyzer D 6100 and probes
- Fluke 39, Handheld Power Meter, Fluke Current Probes

References

[1] Dirk Dietrich, "Investigations in a Hybrid Power System with focus on energy backup and system modelling", Diploma Thesis, Göteborg, 2007

[2] "Security of Energy Supply - The Potentials and Reserves of Various Energy Sources; Technologies Furthering Self Reliance and the Impact of Policy Decisions", ITRE, Bruxelles, Sept. 2006

[3] World Energy Outlook 2002, International Energy Agency (IEA), Paris, 2003

[4] http://www.mccloskeycoal.com, chart for steam cole, from 12.11.2006

[5] http://www.iea.org chart for crude oil, from 12.11.2006

[6] http://de.wikipedia.org/wiki/Uran, historic uranium chart, from 12.11.2006

[7] Jan Linders, Lars Holmblad, "Vind-Dieselsystem: Elforsörjning På Isolerade Platser", Technical Report No. 68L, Göteborg, 1989

[8] Erik Högberg, Per Lundmark, "Design and Test of an Electrical System for a Direct-Driven Permanent-Magnet Generator for a Wind Turbine", Göteborg, 1997

[9] Magnus Carlsson, Jörgen Kjellberg, Ola Carlson, "Utveckling och laboratorieprov av vind-diesel system", Report No. 15R, Chalmers Göteborg, 1999

[10] NOAA Earth System Research Laboratory, "Radiative Climate Forcing by Long-Lived Greenhouse Gases: The NOAA Annual Greenhouse Gas Index (AGGI)", http://www.cmdl.noaa.gov/aggi/, 24.04.2007

[11] http://de.wikipedia.org/wiki/Treibhausgas, from 24.04.2007

[12] "Global Emission Model for Integrated Systems – version 4.14", published by Öko-Institut - The Institute of Applied Ecology, Germany

[13] Asia Pacific Development Power & Energy, "Massive savings on diesel fuel with a PitchWind Hybrid Power System", publication APDPE6, 2002

[14] http://www.wwindea.org/home/index.php, World Wind Energy Association, 31.12.2005

[15] http://de.wikipedia.org/wiki/Windenergie#International, 24.4.2007

[16] http://sv.wikipedia.org/wiki/Vindkraft, 24.4.2007

[17] IAEA Annual Report 2005

[18] http://www.wwindea.org/home/images/stories/pdfs/pr_statistics2006_290107.pdf, WWEA, 29.2.2007

[19] http://de.wikipedia.org/wiki/Solarzelle#Energetische_Amortisation_und_Erntefaktoren, 24.4.2007

[20] Klaus Stratmann, “Solarstrom – teuer und ineffizient” referring to a study from IBW, Handelslatt Online, 24.4.2007

[21] Treibhausgasemissionen und Vermeidungskosten der nuklearen, fossilen und erneuerbaren Strombereitstellung, Öko-Institut, Büro Darmstadt, März 2007

[22] Power Performance Evaluation of Pitch Wind 20kW at Halmdstad 1999-09-07 – 1999-10-26, Jonas Gustavsson, FFA Sweden

[23] A.Grauers, S. Landström, “The Rectifiers Influence on the Size of Direct-driven Generators”, Proceedings of the 1999 European Wind Energy Conference and Exhibition (EWEC’99), Nice, France, pp. 829-832

[24] Martin Bartholet, Christof Zwyssig, “Permanent-Magnet Generator with Series Compensation, Diode Rectifier and DC/DC Converter for Wind Turbine Applications”, Göteborg, Sweden, 2004

[25] N. Mohand, T. Undeland, W. Robbins, “Power Electronics”, Fig. 7-31, pp. 195

[26] Teknisk slutrapport, “Drift av Hönö provstation – HÖNÖ”, Göteborg, 2006

[27] Peter Vas, “Sensorless Vector and Direct Torque Control”, Oxford University Press 1998

[28] N. Mohand, T. Undeland, W. Robbins, “Power Electronics”, chapter 8

[29] http://www.windpower.org Danish Wind Industry Association

[30] Joachim Lindström, “Development of an Experimental Permanent-Magnet Motor Drive” Technical Report No. 312L, Göteborg, 1999

[31] Anders Grauers, “Design of Direct-driven Permanent-Magnet Generators for Wind Turbines”, Technical Report No. 292, Göteborg, 1996

[32] Sonja Lundmark, Course Material of “Electric Drives I”, Göteborg, 2006